Baseline surface- and groundwater monitoring prior to an onshore shale gas operation in the Vale of Pickering, UK

Eleanor Raper[1], David Banks[2,3], Joe Shipperbottom[1], Phil Ham[1*]

[1] Envireau Water, Aske Stables, Richmond, North Yorkshire, DL10 5HG, UK

[2] Holymoor Consultancy Ltd., 360 Ashgate Road, Chesterfield, Derbyshire, S40 4BW, UK. Orcid ID: 0000-0002-4575-504X

[3] School of Engineering, University of Glasgow, James Watt Building South, Glasgow G12 8QQ, UK.

[*] Corresponding author: Phil Ham, email PhilHam@envireauwater.co.uk, Tel: 07920 884103

Emails:

ER: ec.raper@hotmail.co.uk

DB: david@holymoor.co.uk

JS: JoeShipperbottom@envireauwater.co.uk

PH: PhilHam@envireauwater.co.uk

Conflict of interest

ER, JS and PH have, via Envireau Water, acted as consultants to Third Energy Ltd. DB has, via Holymoor Consultancy Ltd., acted as consultant to Envireau Water and to Third Energy Ltd. The University of Glasgow has partially funded DB's time in preparing this paper, but declares no known conflict of interest.

Author contributions

ER: data analysis and interpretation, figure preparation, editing of manuscript

DB: preparation of manuscript and figures, data analysis and interpretation

JS: field work, editing of manuscript

PH: editing of manuscript, project management

Baseline surface- and groundwater monitoring prior to an onshore shale gas operation in the Vale of Pickering, UK

Eleanor Raper[1] David Banks[2,3] Joe Shipperbottom[1], Phil Ham[1*]

[1] Envireau Water, Aske Stables, Richmond, North Yorkshire, DL10 5HG, UK

[2] Holymoor Consultancy Ltd., 360 Ashgate Road, Chesterfield, Derbyshire, S40 4BW, UK. Orcid ID: 0000-0002-4575-504X

[3] School of Engineering, University of Glasgow, James Watt Building South, Glasgow, G12 8QQ, UK.

[*] Corresponding author: Phil Ham, email PhilHam@envireauwater.co.uk, Tel: 07920 884103

Abstract

A comprehensive programme of baseline groundwater hydrochemical monitoring has been carried out in connection with the proposed hydraulic fracturing of a 2 to 3 km deep Bowland Shale gas reservoir in borehole KM8 at Kirby Misperton, North Yorkshire, UK. The monitoring infrastructure encompassed: five on-site boreholes with hydraulically open intervals ranging from shallow weathered cover to a c. 200 m deep Corallian limestone aquifer, six off-site wells (hydraulically open in superficial materials and/or Kimmeridge Clay) and four surface water monitoring stations. Groundwater chemistry was high stratified with depth, ranging from slightly acidic, fresh, very hard Ca-HCO_3-SO_4 waters in shallow weathered cover, to brackish, calcium-depleted, highly alkaline waters in the Corallian aquifer. Dissolved methane was detected in most boreholes, with 10 µg/L being typical of shallow boreholes and around 50 mg/L in the Corallian. Low ethane concentrations and isotopic evidence suggest that the methane was predominantly microbial in origin (carboxylate fermentation at shallow depth, natural methanogenic CO_2 reduction at greater depth). Elevated dissolved ethane (20-30 µg/L) was found in one well of intermediate depth, suggesting admixture of a possible thermogenic component, although this could be derived directly from the Kimmeridge Clay penetrated by the well.

1. BACKGROUND

The practice of hydraulic fracturing for stimulation of shale gas wells ('fracking') has attracted considerable controversy amongst the public and academia in recent years. Concerns include issues ranging from (a) additional extraction of new fossil fuel and eventual carbon emission, (b) induced seismicity, (c) local traffic, noise and visual impact to (d) hydrogeological issues. These hydrogeological concerns include potential for groundwater or surface-water contamination (e.g. from subsurface migration of natural brines or introduced chemicals, or from surface fuel or chemical spillages) and the migration of natural gas along wellbores or fracture pathways.

Rigorous scientific studies documenting widespread and/or systematic groundwater contamination from such activities are remarkably few (Osborn et al. 2011, Vengosh et al. 2013, Warner et al. 2013, Catalyst 2016). A major review by the USEPA (2016) lists certain scenarios where hydraulic fracturing for hydrocarbons can have hydrogeological impacts, and some cases are documented where well integrity failure was suspected to have negatively impacted groundwater quality (Bair et al. 2010, Darrah et al. 2014, Jackson et al. 2013a, USEPA 2015, USEPA 2017). The apparent disconnect between the findings of scientific studies and the concerns of opposition groups highlights the need for pre-exploitation understanding of natural groundwater quality. In the public consciousness there is a common impression that groundwater is pristine, sterile and safe to drink. In reality, hydrogeologists know that groundwater is not so, and may naturally contain problematic solutes such as arsenic, fluoride, radon or uranium, as studies from the UK (Middleton et al. 2016), Scandinavia (Banks et al. 1995, 1998, Frengstad et al. 2000) and Bangladesh (Shankar et al. 2014, Ahmad et al. 2018, Ali et al. 2019) illustrate. It has also been recognised that dissolved hydrocarbons (e.g. methane) are found as a naturally-occurring component of many groundwater systems in the UK (Gooddy & Darling 2005, Darling & Gooddy 2006, Bell et al. 2016, 2017, Teasdale et al. 2018) and elsewhere (Schloemer et al. 2016).

It is understandable that residents near a hydrocarbon exploitation site will suddenly take an interest in their groundwater supplies and start to analyse them. When undesirable solutes are found in the water, it is a natural human reaction to ascribe them to industry, rather than to nature. This experience should underline the absolute need to undertake pre-operational baseline surveys of water quality (Mair et al. 2012, Vidic et al. 2013, Jackson et al. 2013b, Smedley et al. 2017), to ascertain whether changes take place due to hydrocarbon exploitation operations and whether any undesirable solutes in the water have their origin in natural processes or contamination. The European Union SHEER project developed a code of practice for water monitoring prior to, during and after unconventional hydrocarbon exploitation, which demonstrated the implementation of this methodology at a shale

94 gas hydraulic fracturing site at Wysin, Poland (SHEER 2018, Montcoudiol et al. 2019). Data from the
95 Kirby Misperton site in the Vale of Pickering, North Yorkshire was also used in 2017 to propose a
96 methodology for baseline development in a UK context (Hood et al. 2017).

97 This paper describes the pre-stimulation surface- and ground-water monitoring carried out on behalf
98 of the operator of the Kirby Misperton KM-8 well in the Vale of Pickering, North Yorkshire, UK (Figure
99 1). It was proposed to carry out hydraulic fracturing of this well in the Namurian Bowland Shale to
100 facilitate the production of shale gas. The baseline monitoring continued for a considerable period, in
101 anticipation of approval being granted to commence hydraulic fracturing operations. In fact, hydraulic
102 fracturing and production of shale gas were not implemented at the site, and at present there is a
103 moratorium on hydraulic fracturing for shale gas exploitation in England (Ambrose 2019, UK
104 Government 2019).

105 This paper does not seek to defend or oppose the practices of onshore shale gas exploitation in the
106 UK, nor that of hydraulic fracturing in such contexts. It does, however, present the data set collected
107 (which can be regarded as a pre-fracking baseline data set) from the Kirby Misperton site, as it
108 elucidates the complexities of representative data collection and also sheds light on the high
109 concentrations of (natural) hydrocarbon gases than can exist in undisturbed British groundwater.

110

2. THE SITE

Kirby Misperton lies in the Vale of Pickering, in the English county of North Yorkshire (Figure 1). The Vale of Pickering is a broad topographic depression between the North York Moors in the north, the Hambleton Hills in the west, the Howardian Hills to the south-west (all of which are formed by rocks of the Jurassic age Corallian Group) and the Yorkshire Wolds in the south-east (Cretaceous Chalk). The Vale is drained by a number of a tributaries of the River Derwent, including the Rivers Riccal, Seven, Dove and Rye. The land-use is predominantly arable farming. The annual rainfall is 717–987 mm year^{-1} (based on the 1961-1990 averages) and typically contains (in 2007) around 3 mg L^{-1} Na^+ and 5 mg L^{-1} Cl^-. These concentrations are believed to be multiplied around three-fold by evapotranspiration in the soil zone during groundwater recharge (Bearcock et al. 2015).

The Pickering area contains some of the UK's more important onshore natural gas reservoirs, predominantly associated with Permian Zechstein Group carbonates (Haarhoff et al. 2016, 2018). These fields were originally operated by Candecca Resources (owned by BP), were transferred in 1992 to Kelt (UK) and were taken over by Viking Petroleum UK in the 2000s. Viking Petroleum changed its name to Third Energy in 2013. The conventional fields supply gas to an electricity generating station at Knapton. Two of the operational sites are located at Kirby Misperton: the Kirby Misperton A (KMA) and Kirby Misperton B (KMB) sites.

The KMA site (Figure 2) is of rectangular shape, bunded, at an elevation of c. +30 m above sea level (m asl) and is surrounded by predominantly arable farmland. A small intermittently flowing drain, the Sugar Hill Drain, rises near the outskirts of Kirby Misperton village, runs southward along the western boundary of the site, and eventually discharges into the Costa Beck, a tributary of the River Derwent.

In 2013, Third Energy drilled a new near-vertical well (KM-8) to 3099 m TVD (true vertical depth) into the Carboniferous strata underlying the conventional Permian reservoirs at KMA (grid reference SE 7712 7897). A plan was developed to hydraulically fracture the well at five intervals between approximately 2123 m and 3044 m TVD to ascertain whether natural gas could be produced from the Carboniferous Bowland Shale Formation (Envireau Water 2017a, Third Energy 2017). Given the controversy surrounding shale gas exploitation, and as the Vale of Pickering was one of several UK areas being considered for this type of operation, the British Geological Survey also carried out regional baseline monitoring in the Vale of Pickering (Smedley et al. 2017). They reported finding a wide range of hydrochemistry, but prevailing reducing redox conditions and dissolved methane of up to 37 mg/L in the shallow strata of the area. The data set reported in this paper represents the baseline and pre-operational monitoring carried out by the operator to fulfil regulatory obligations. It is recognised that the term "baseline" could be misleading here: the monitoring reported in this paper

commenced in 2017, long after well KM-8, and the other conventional gas wells (KM-1 and KM-3) present at the KMA site, were drilled. The data set thus cannot conclusively answer the question of whether the drilling of these wells led to any impact on the hydrogeological environment: the monitoring program was designed to document conditions before and during the proposed hydraulic fracturing of KM-8. In reality, the monitoring commenced in April 2017, three months before preparatory work at the KM-8 wellhead, and continued while equipment and materials were moved onto site in preparation for hydraulic stimulation. As has been noted above, for various reasons, the hydraulic fracturing never took place and we can thus regard the entire data set as a "local baseline" which supplements and informs the regional British Geological Survey studies.

2.1 Geological Context

The Vale of Pickering was occupied during the late Devensian by a glacial ice-dammed lake ("Lake Pickering"), or series of such lakes. The area of the former Lake is blanketed with a cover of laminated glaciolacustrine clays and silts, with some sands. Silty and sandy material become more prominent towards the top of the sequence. At the edge of the palaeo-lake, rivers built out deltas, which are now reflected as fringes of glaciofluvial sands and gravels around the margins of the Vale. Just beyond the edges of Lake Pickering and in small topographic highs in the central Vale (former islands), the underlying Jurassic age Kimmeridge Clay Formation is exposed, sometimes draped with remnants of mid-Pleistocene tills. Indeed, KMA lies on one such "island" within the surrounding Lake Pickering lacustrine deposits (Ford et al. 2015, Powell et al. 2016). The Pleistocene deposits have been subsequently incised by the River Derwent and its tributaries, which have deposited strips of alluvium along the modern river valleys. The total Quaternary cover in the Vale of Pickering can be up to 35 m thick (Ford et al. 2015, Evans et al. 2017, Lincoln et al. 2017).

The Vale is largely underlain by the upper Jurassic Kimmeridge Clay Formation (a member of the argillaceous Ancholme Group), a locally silty or sandy fossiliferous marine mudstone, which contains thin siltstone or cementstone beds and which can be calcareous and have a high kerogen content (Williams 1986, Trebovillard et al. 1994, BGS 2020). Published mapping does not differentiate between the Kimmeridge Clay Formation and the underlying Ampthill Clay formation which forms the lower portion of the Ancholme Group (BGS 2000) and the term Kimmeridge Clay Formation will be used to describe the combined unit in this paper. This overlies the Corallian Group, which comprises the 9-15 m thick Upper Calcareous Grit Formation (a fine calcareous sandstone), overlying the Corallian Oolite Formation (50-58 m thick, dominated by oolitic limestones with some calcareous sandstones and shelly limestones), in turn overlying the Lower Calcareous Grit Formation (15-50 m thick). The Corallian

177 Group is underlain by the 20-50 m thick Upper Jurassic argillaceous Oxford Clay Formation (BGS 2000,
178 Bearcock et al. 2015). Below this is a thick and variable sequence of Jurassic, Triassic and Permian
179 sedimentary rocks. The monitored formations (i.e. down to the Corallian) are thus located a
180 considerable distance above the Carboniferous Bowland Shale reservoir target (2 to 3 km depth).

181 The Corallian Oolite Formation represents a significant aquifer in the area, whose properties and
182 hydrochemistry are summarised by Reeves et al. (1978), Allen et al. (1997) and Bearcock et al. (2015).
183 Its hydrochemistry evolves from fresh Ca-HCO_3 groundwater in outcrop and recharge areas to Na-
184 HCO_3 waters as it becomes more confined.

185

3. THE MONITORING REGIME

A range of monitoring activities was required in order for Third Energy to operate KMA and to plan the hydraulic stimulation of KM-8: these included a baseline soil quality survey, a survey of near surface methane concentrations, monitoring of induced seismicity and surface vibration, regular physical inspection of containment infrastructure, monitoring of noise, air quality, natural radioactive substances in aqueous waste streams and onsite gas monitoring (Third Energy 2017a,b; Environment Agency 2017). A programme of surface- and groundwater monitoring was also designed and implemented to meet conditions of the permit issued by the Environment Agency (2016) in accordance with the Environmental Permitting (England & Wales) Regulations 2010. The regulatory and consultation history can be traced via the Environment Agency's (2020) online consultation hub. This study reports the results from the surface water and groundwater component of the monitoring programme, from April 2017 to June 2018, with extended sampling of on-site wells for methane only to September 2019. The paper reports only the inorganic chemical and dissolved light hydrocarbon monitoring data from the study. The full range of other parameters (e.g. organic parameters, not reported here) monitored in the groundwater, in accordance with the EA permit, are listed in Table 1.

3.1 Surface Water Monitoring Stations

Four surface water sampling stations were established. S4 and S1 were the upstream and downstream locations on the Sugar Hill Drain, immediately north and south of KMA (Figure 2). The Sugar Hill Drain is part of a large field drainage system, draining terrain comprising low permeability glacial till, glaciolacustrine deposits and the Kimmeridge Clay Formation. S3 was established on the Ackland Beck (22 m asl) and S2 on the Costa Beck (22 m asl), which is the largest of the monitored watercourses. Reported surface water data stretch from April 2017 to May 2018.

3.2 On-Site Groundwater Monitoring Infrastructure

Five groundwater monitoring boreholes were drilled within KMA in late 2015 (Envireau Water 2017a), as shown in Figures 2 and 3 and summarised in Table 2. Three of the boreholes (BHA-C) were 11.5 m deep, with slotted screen straddling the water table within the thin layer of superficial Quaternary deposits and weathered Kimmeridge Clay. The rest water level in these boreholes was 9.04 to 9.52 m below well top (23.03 to 23.37 m asl) in April 2016.

217 BHD was drilled to 38 m depth and monitors groundwater conditions within the interval 25 to 37 m
218 bgl, within the unweathered portion of the Kimmeridge Clay Formation. The rest water level in BHD
219 was 7.26 m below well top (22.38 m asl) in April 2016.

220 The deep BHE monitors groundwater conditions within confined Corallian aquifer in an open hole
221 interval between 193 and 222 m bgl (-163 to -192 m asl). The rest water level in BHE was 3.01 m below
222 well top (26.72 m asl) in April 2016, and the water characteristically evolved visible bubbles of
223 methane gas, when pumped. Note that static water levels become shallower as the wells become
224 deeper, suggesting a generally upwards hydraulic head gradient.

225 Reported data from BHA-BHE cover the period from April 2017 to June 2018, with analyses for
226 dissolved methane extending to September 2019.

227

228 **3.3 Off-Site Groundwater Monitoring Infrastructure**

229 Six off-site wells and boreholes (G1 to G6) were identified at farms and private properties within an
230 approximate 2 km radius of the well site. These wells and boreholes all occur in a similar geological
231 situation: depths varied between c. 5 m (G5) and possibly as much as 50 m bgl (G3 and G4). They are
232 typically installed into Pleistocene lacustrine sediments (of the glacial Lake Pickering) and/or the upper
233 section of Kimmeridge Clay. Reported data from the off-site wells cover the period from April 2017 to
234 April 2018.

235

4. METHODS

4.1 Sample aliquots and analysis

Sampling was carried out with reference to *British Standard ISO 5667 - Water Quality Sampling.* Sample containers for analytical parameters listed in Table 1 were provided by a UKAS accredited laboratory: Element Materials Technology (formerly known as Jones Environmental Laboratories and Exova Jones Environmental).

In the field, sample containers which did not include preservatives were pre-rinsed with sample water. Sample containers were filled ensuring that no headspace was present. The following aliquots are typical of those taken during each sampling round:

- 100 ml polyethylene flask, unfiltered but with H_2SO_4 preservative (1 ml of 19% H_2SO_4) , for determination of ammoniacal nitrogen.
- 4 x 40 ml glass vials, with a polypropylene cap and silicone/PTFE septum, for dissolved gases and other volatile organic analyses. Water for these aliquots was unfiltered and unpreserved. Vial was filled to top, ensuring there was no headspace.
- 100 ml polyethylene flask, for dissolved metals. Water for these aliquots was filtered using a 0.45 µm syringe-mounted filter in the field. Nitric acid was then added to the sample aliquots (1ml of 22% HNO_3) to prevent metal sorption and precipitation during transport and storage.
- 500 ml polyethylene flasks, with samples being unfiltered and unpreserved, for anions and other parameters.
- Additional aliquots in various glass flasks for organic parameters (not discussed in this paper).

At the laboratory, the following methods were employed for determination of inorganic parameters in the water samples:

- Total dissolved solids: by gravimetric determination based on a modified BS 1377-3 1990 / USEPA 160.3 methodology.
- Total suspended solids: by filtration, drying of residue and gravimetric determination, based on a modified USEPA 160.2 methodology.
- Dissolved metals: by inductively coupled plasma optical emission spectrometry (ICP-OES), based on modified USEPA 200.7 and 6010B and BS EN ISO 11885 2009 methodologies.

- Sulphate, chloride, nitrate, phosphate, ammoniacal nitrogen: by soluble ion analysis using a Thermo Aquakem Photometric Automatic Analyser, based on modified USEPA 325.2, 375.4, 365.2, 353.1 and 354.1 methodologies.
- pH, alkalinity and electrical conductivity: by Metroohm automated probe and automated titration analyser.

Methods for other parameters not reported in this paper (e.g. organic compounds) can be found in Envireau Water (2017b), available via Environment Agency (2020).

4.2 Surface water sampling

Surface water samples (S1 to S4) were obtained by the use of a sampling pole and clean collection vessel, rinsed with distilled water between monitoring sites to prevent cross-contamination. Samples were collected to target the major flow route of the waterbody (i.e., mid-stream, where possible). Sample water was decanted from the collection vessel into the appropriate sample containers (as described above) provided by the laboratories. Field determinations of pH, electrical conductivity (EC), temperature and oxidation-reduction potential (ORP) were made immediately using a calibrated In-Situ SmarTROLL multiparameter device. The ORP was measured using a Pt:Ag/AgCl electrode combination. According to Striggow (2013), an ORP determined by such an electrode can be converted to Eh by adding 214 to 220 mV to the ORP value at 10°C, depending on electrolyte strength.

4.3 Groundwater sampling

Samples were obtained from off-site wells (G1 to G6) either: (i) from the well's installed pump (many of the wells serve private farms or residences), or (ii) from the first available tap along the well's pipe network (but prior to any treatment system), or (iii) via the use of a disposable single valve bailer. Samples were collected, following a period of purging, directly into the appropriate sample containers or, if this was not possible, decanted from a larger collection vessel directly into the sample container. Field chemistry measurements (pH, EC, ORP, temperature) were made immediately using an In-Situ SmarTROLL multiparameter device.

For the five on-site boreholes (BHA to BHE), dedicated low-volume pneumatic bladder pumps were installed in each on-site borehole. Water was discharged at the surface (via the action of a compressor on the downhole bladder) at a rate of c. 1 L minute^{-1} through a flow-through cell accommodating the SmarTROLL multi-parameter device. Water chemistry parameters (pH, EC, ORP, temperature) were

297 monitored until stable conditions were achieved, which often took 20-25 minutes. Upon stabilisation
298 of the field parameters, the flow-through cell was uncoupled and samples were collected directly from
299 the discharge line of the bladder pump into sample containers.

300

301 **4.4 Dissolved methane sampling**

302 Two different sampling methods were employed when monitoring for dissolved methane: the
303 project's standard methodology and (on selected samples from BHE) the British Geological Survey's
304 "steel cylinder" method ("BGS method"; Bell et al. 2016, 2017, see below).

305 The project's standard methodology simply involved the filling of 40 ml vials (glass, with polypropylene
306 caps and silicone/PTFE septa) directly from the sample line or discharge. For the on-site boreholes
307 (BHA-BHE), the vials were filled, following stabilisation of field parameters, directly from the discharge
308 line of the bladder pump, ensuring that no headspace was present, and sealed. For off-site wells and
309 surface waters, water was collected in the sample vials from the discharge or sample container and
310 then sealed. The vials were inverted when in transit to the laboratory to minimise the risk of gas loss
311 through the cap of the vial.

312 Between April 2017 and April 2018, samples of groundwater for dissolved methane analysis were
313 taken from borehole BHE (the borehole with the highest dissolved methane concentration) using both
314 the project's standard methodology, and additionally the "BGS method". This involved pumping
315 groundwater through a double valved steel cylinder (or "bomb") of c. 50 cm^3 volume (Bell et al. 2016,
316 2017), while endeavouring to ensure that that no gas bubbles adhered to the walls of the cylinder or
317 connecting tubing, by constantly knocking the tubes and cylinder with a metal tool. After a bubble-
318 free, steady flow had been established through the cylinder, and it had been adequately flushed, a
319 volume of water was sealed in the cylinder by progressively closing the cylinder inflow and exit valves.

320

321 **4.5 Dissolved methane analysis**

322 Samples collected for dissolved methane using the "Project method" were returned to the laboratory
323 for analysis of methane, CO_2 and other light hydrocarbons using their method TM25, using a
324 headspace gas chromatograph / flame ionisation detector (GC/FID) technique. This technique had a
325 reporting limit of 1 µg/L, although some blank samples exhibited false detects in the range 3 to 10
326 µg/L (see Figure 5 and Section 5.1) and the realistic limit of quantification is likely within that range.

Duplicates of selected samples were also sent to Department of Earth Sciences, Durham University, UK, for stable isotope analysis on dissolved methane and CO_2. The analytical method employed by Durham University was based on Roberts & Shiller (2015).

The sealed steel cylinders resulting from the "BGS method" were returned to the British Geological Survey's Wallingford laboratories. The contents were subsequently analysed by the BGS Wallingford laboratories, also employing a headspace gas chromatograph / flame ionisation detector (GC/FID) technique, described by Bell et al. (2017), involving the transfer of the water from the cylinder to a c. 120 cm^3 evacuated glass bulb using helium gas. The headspace gas was then admitted, via the evacuated inlet system of the GC, to a 3.2 mm diameter Porapak-Q packed column at room temperature. Eluting methane was detected by flame ionisation detection, with a detection limit of c. 0.5 µg/L.

4.6 Quality control

For every sampling round, at least one sample point was selected for collection of duplicate samples for every parameter, using identical sampling and preservation methods. These were analysed and compared with the results of every parameter.

For every sampling round, a set of sample aliquots was prepared in the field using high purity distilled water, again using identical sample flasks and preservations to the primary water samples.

For every water sample, an ionic balance was calculated between cations and anions as milliequivalents per litre (meq L^{-1}) of charge.

At the carbon isotope laboratory, control samples of laboratory air and laboratory tap water were analysed, as part of the laboratory's standard practice.

5. RESULTS

5.1 Quality Control

In the duplicate samples taken every sample round, analytical reproducibility was found to be very good for all non-gaseous dissolved inorganic species.

For dissolved methane reproducibility was also found to be remarkably good, given the simplicity of the project's standard sampling method, especially at high concentrations (Figure 4). At concentrations of around 10 µg/L, reproducibility was noticeably worse, suggesting that this was the limit of reliable determination of dissolved methane in our samples (despite the cited analytical detection limit of 1 µg/L). Overall, very good reproducibility was found for the results of dissolved CO_2 analysis (Figure 4).

Ethane was only detected in significant quantities in duplicate sets of samples from borehole G3, at concentrations of around 20-30 µg/L. However, the reproducibility was also very good. In a single sample, which returned lower concentrations, reproducibility was poor (Figure 4).

Ionic balances were calculated for all samples and were generally found to be within acceptable limits. Of 185 samples in total, 134 (72%) had an ion balance error (IBE) of less than ±6%, and 179 (97%) less than 10%, based on the major ion parameters Na^+, Ca^{2+}, Mg^{2+}, K^+, NH_4^+, NO_3^-, SO_4^{2-}, Alkalinity (HCO_3^- + CO_3^{2-}) and Cl^-. The largest calculated IBE was 27%.

As regards the blank samples prepared from distilled water during each sampling round, and submitted with the rest of the samples, very few issues were experienced with false detects. Where occasional detects were located, these were queried with the laboratory and resolved. (For example, a series of minor boron detects were found in blank samples in the period Nov. 2017 to Jan. 2018, and traced back to issues with the stock acid used to preserve samples – e.g. prolonged acid storage in borosilicate glass. Reported boron concentrations close to the detection limit - i.e. approximate range 12 -20 µg/L - should thus be treated with caution).

As regards dissolved gases, the blank concentration for methane was typically around the detection limit of 1 µg/L (median 1 µg/L, 75% percentile 3 µg/L), occasionally reaching as high as 18 µg/L (see Figure 5). No detects of ethane were found in the blank samples.

As regards the control samples for carbon isotope analysis, the laboratory air effectively reflected global atmospheric methane signatures, with a $\delta^{13}C$ of -50‰ being consistently reported. We regard the laboratory tap water as being of limited utility as a control, as the origin of the water is not known; it returned typical $\delta^{13}C$ of -49 to -50‰, probably reflecting equilibration with atmospheric methane.

381

382 **5.2 Methane sampling method**

383 Despite the good overall internal reproducibility of the project sampling method over a range of
384 methane concentrations, comparability with the BGS method was rather poor (Figure 6). Although
385 some degree of correlation was observed between the two methods, the BGS method did return some
386 very low methane concentrations, despite the consistently high methane determinations resulting
387 from the standard project methodology.

388 In this particular hydrogeological situation, we regard the standard project method as being more
389 reliable and reproducible than the BGS method. There may, however, be extenuating circumstances
390 for the poor performance of the BGS methodology at BHE – namely (i) the very low flow rates achieved
391 by the installed bladder pump (arguably inadequate to efficiently purge the cylinder) and (ii) the
392 observed exsolution of methane gas from the water and the tendency of it to adhere to sample tubing.

393

394 **5.3 Surface Water Chemistry**

395 The waters sampled from the surface water stations were all typically calcium bicarbonate waters
396 (Figure 7), which show considerably more seasonal and temporal chemical variation than do the
397 groundwaters. Statistical summaries of field and laboratory determinations are provided in Tables 3a
398 and 3b, cited as median values and the interquartile (25-percentile to 75-percentile) range (IQR). Such
399 a non-parametric method of presentation has been used throughout: this is widely favoured as a
400 means of presenting geochemical data, over mean ± standard deviation, as the latter makes
401 assumptions about data symmetry and normality seldom present in geochemical data sets (Reimann
402 & Filzmoser 2000).

403 All sampled streams contained slightly alkaline, relatively ion-rich water (EC typically >500 µS/cm,
404 alkalinity > 4 meq/L, calcium >80 mg/L). Redox conditions were oxidising and temperatures exhibited
405 the expected seasonal trend. S1 and S4 (Sugar Hill Drain) were typically dry during summer months,
406 so data are skewed towards winter conditions. S1 and S4 showed a considerable degree of co-variation
407 in water quality, being located on the same stream, located down-gradient and up-gradient of the well
408 site, respectively.

409 Chloride concentrations in S2 were around 30 mg/L, while those in in S1, S4 and (especially) S3 were
410 somewhat higher, typically at 40 – 80 mg/L. Variations in sodium broadly corresponded to those in
411 chloride.

During the sampling period, nitrate concentrations showed a tendency to decrease in S2, S3 and S4, although a period of elevated concentrations of up to 40-50 mg/L (as NO_3^-) was observed in S1 and S4 in October - November 2017. Concentrations of ammoniacal nitrogen were generally extremely low in the surface waters (< 0.2 mg/L as N), with the exception of a brief period in March-April 2018, when elevated ammoniacal nitrogen (over 2 mg/L as N in March) was observed in S1 and S4, coinciding with slightly elevated dissolved iron, elevated potassium (up to 26.8 mg/L in March) and low nitrate.

Stream sampling point S2 exhibited consistent detects of methane at around 10 µg/L, while sporadic detects of a similar magnitude were observed in S3. Locations S1 and S4 returned methane concentrations typically below detection limit (< 1 µg/L) with occasional positive detects.

5.4 Off-site shallow wells G2-G6

Wells G2 to G6 were sampled between April 2017 and April 2018 (Tables 4a, 4b). The groundwater chemistry at all the sites was a strongly sodium-bicarbonate dominated water type (Figure 7).

G2, G4, G5 and G6 exhibited low calcium concentrations of 20-30 mg/L, sodium in the range 140-280 mg/L, sulphate around 20-170 mg/L, chloride 20-30 mg/L, low nitrate (typically < 2 mg/L as NO_3^-), electrical conductivities of 600-1100 µs/cm and alkalinities of 6-10 meq/L. Ammoniacal nitrogen concentrations were around 0.7 mg/L (as N) in G2, G4 and G5 and somewhat lower in G6.

G3, one of the deeper wells (c. 50 m deep), distinguished itself by a slightly different chemistry in respect of some parameters, with especially high sodium (350-400 mg/L), chloride (40-50 mg/L), sulphate, alkalinity (>12 meq/L) and ammoniacal nitrogen (around 1.2 mg/L as N).

Dissolved methane concentrations in G3 were consistently high at 1 to 4.7 mg/L. In G2, G4, G5 and G6, median dissolved methane was typically in the range 11-21 µg/L, with concentrations as high as 34 and 63 µg/L recorded, respectively in G2 and G6. Ethane was detected at concentrations of up to 20 µg/L in G3, these being the highest ethane concentrations observed at any monitoring point.

5.5 On-site shallow boreholes BHA - BHC

The shallow on-site boreholes, BHA, BHB and BHC, all exhibited a slightly acidic, Ca-HCO_3-SO_4 water chemistry (Table 5a, 5b, Figure 7). Sodium concentrations were typically in the range 25-40 mg/L, slightly higher than the surface waters. Chloride increased from BHA (around 30 mg/L) to BHC (c. 60 mg/L) and exceeded 100 mg/L in BHB. Alkalinity and water hardness were very high, at typically > 8

meq/L and >15 meq/L, respectively. Nitrate concentrations, as in the off-site groundwaters, were surprisingly low for such an agricultural area (typically <0.2 mg/L as NO_3^-).

5.6 Intermediate on-site borehole BHD, and off-site well G1

BHD extended into the upper section of the pyrite- and organic-rich Kimmeridge Clay Formation. The pH was higher and sulphate concentration slightly lower than in BHA, B and C. Most notably, the alkalinity was extremely high (around 13 meq/L) and calcium concentrations low (< 50 mg/L). The cationic composition was dominated by sodium, giving an overall Na-HCO_3 water type (Figure 7). Chloride concentrations (c. 45 mg/L) were modest, comparable to surface waters and shallow groundwaters. Reducing conditions were evidenced by lack of nitrate, ammoniacal nitrogen at around 1.4 mg/L (as N) and negative ORP. Methane was consistently detected in the water from BHD at several tens of µg/L (typically 60-80 µg/L). The water chemistry showed little temporal fluctuation. Boron concentrations were consistently high (c. 1.5 mg/L) in this groundwater.

Borehole G1 exhibited many hydrochemical similarities to BHD. It had a slightly alkaline pH and a negative ORP. Calcium concentrations were modest (60-70 mg/L), while alkalinity and sodium were both high (c. 13 meq/L and c. 640 mg/L). While chloride was slightly elevated (c. 100 mg/L), the sodium was greatly in excess of chloride. Sulphate concentrations were considerably higher than BHD, at 800-840 mg/L. Nitrate was effectively absent from the water, while ammoniacal nitrogen was present at c. 2.3 mg/L. As in BHD, boron was present in high concentrations (2.3 mg/L), as was strontium (c. 4 mg/L). Methane was typically detected at around 570-710 µg/L.

5.7 Deep (Corallian) on-site borehole BHE

The deep borehole BHE extends through the Ancholme Group to the Corallian Oolite. The groundwater was brackish (EC > 3000 µS/cm), of sodium chloride composition, with sodium concentrations (typically c. 750 mg/L) being slightly in excess of chloride (typically c. 680 mg/L). The pH was extremely high (just below 10) and the ORP strongly negative. The alkalinity was also very high at around 11 meq/L. Sulphate was also almost absent from the water, as were dissolved iron and manganese. The water consistently contained abundant methane (c. 50 mg/L), and traces of ethane (5-10 µg/L).

5.8 Carbon isotopic data from dissolved methane and CO_2

473 The $\delta^{13}C$ results for the dissolved methane and carbon dioxide are summarised in Table 6. Most
474 samples returned a dissolved methane $\delta^{13}C$ of around -50 ‰ (which is similar to the global
475 atmospheric methane signature and the laboratory air samples used as control). BHE, however,
476 exhibited a consistently low methane $\delta^{13}C$, typically around or below -70‰. G1 and G3 returned a
477 range of methane $\delta^{13}C$ results, but with at least 25% of values below -65‰.

478 Most samples returned a dissolved carbon dioxide $\delta^{13}C$ of around -26‰. BHE, however, exhibited a
479 consistently higher carbon dioxide $\delta^{13}C$, typically around or below -13 to -8‰.

480

6. INTERPRETATION - HYDROCHEMISTRY

6.1 Surface Waters

The surface waters showed a hydrochemical variation reflecting greater responsiveness to temporal patterns in climatic, rainfall and land use factors than groundwater. The fact that S2 exhibited a lower degree of temporal variation than the other surface water sampling points reflects its location on a higher order stream with a larger flow than the other monitoring sites. S2 thus integrates flows from a number of lower order streams and is less likely to be susceptible to very rapid water chemistry and climatic fluctuations. Nevertheless, the sampled streams all contained relatively ion-rich water (electrical conductivity typically >500 µS/cm, alkalinity > 4 meq/L, calcium >80 mg/L), characteristic of a high component of groundwater baseflow. The fact that pH was slightly alkaline and higher than most of the shallow groundwaters probably reflects degassing of acidic CO_2 from groundwater baseflow on entry to surface waters.

The modest chloride concentrations in S2 (c. 30 mg/L) were somewhat higher than the 11-12 mg/L (Shand et al. 2002) that can be explained by the content of marine salts and industrial chloride in evapotranspiratively concentrated rainfall. Cape et al. (2014) report median and 75-percentile concentrations of c. 3 mg/L and 5 mg/L, respectively, for the period 1986-2011 at rainfall stations at Thorganby and High Muffles. The higher chloride concentrations in S1, S4 and S3 suggest an additional source of chloride in these catchments – possible candidate sources could include agricultural fertilisers, small quantities of sewage effluent or even road salts (Granato et al. 2015, Rivett et al. 2016).

During winter 2017-2018, the Sugar Hill Drain samples S1 and S4 both experienced a period of several sample rounds when elevated dissolved iron was observed, reaching values of over 500 µg/L in December and January. This may represent periods of waterlogged soil conditions, causing reducing conditions and mobilisation of iron in dissolved form, or increased run-off of humic compounds from organic moorland soils.

There were also episodes of elevated nitrate in the Sugar Hill Drain (especially October-November 2017), probably representing flushing of nutrients from agricultural soils by rainfall recharge. The episode of elevated ammonium, iron and potassium in March-April 2018 (coupled with low nitrate) probably also has an agricultural source: e.g. a release of organic manure could create ammonium-rich, reducing conditions in the stream. In all cases where episodes of elevated iron, ammonium, potassium or nitrate were observed, the elevated concentrations occurred in S4 (upstream of operations site) as well as S1 and could not be ascribed to activities at the site.

513 The dissolved methane concentrations detected in the surface waters were too low to perform
514 reliable isotopic determinations. The source of the methane in the surface waters remains
515 undetermined.

516

517 **6.2 Shallow off-site wells G2-G6**

518 The samples from the off-site wells G2-G6 (within c. 2 -3 km of KMA) all exhibited broadly similar water
519 chemical characteristics, which is surprising given the varied geographical situations, well installations,
520 and land uses.

521 The chloride concentrations in these groundwaters were similar to the surface waters and consistent
522 with other shallow groundwaters and surface waters in the central UK (Banks 1997). The calcium
523 concentrations were much lower and the sodium concentrations were much higher than the surface
524 waters. This may reflect the surface waters being fed by carbonate-rich aquifer baseflow, while G2-
525 G6 were in silicate-dominated lithologies, or it may reflect aquifer processes such as calcite
526 precipitation and sodium silicate hydrolysis, or cation exchange. The sodium bicarbonate water
527 chemistry is usually characteristic of a high degree of water-rock interaction (Frengstad & Banks 2000,
528 Banks & Frengstad 2006).

529 The low nitrate concentrations in such an agricultural area suggest either a lack of modern recharge
530 or denitrifying processes under mildly reducing conditions (Rivett et al. 2008). This was especially so
531 in G3, where the elevated hydrocarbon contents and ammonium concentration suggest more
532 reducing conditions.

533 The methane content in these groundwaters was variable, which may reflect varying well construction
534 factors and sampling equipment as much as geological factors, although G3 did display consistently
535 higher detects of methane and ethane.

536

537 **6.3 Shallow on-site wells BHA-BHC**

538 The lower pH, high alkalinity, and high calcium and sulphate in the groundwaters from these boreholes
539 are unusual and completely different from the shallow off-site groundwaters. One plausible
540 explanation is that the water chemistry owes its characteristics to either oxidation of sedimentary
541 pyrite or dissolution of secondary selenite / gypsum derived from Kimmeridge Clay Formation or
542 glacial till which are exposed in the vicinity (Cope 1974, Tribovillard et al. 1994, Gallois 2004). This
543 would release sulphate and protons, which could then subsequently dissolve calcite to release calcium

and carbonate. The low pH and high alkalinity also account for the very high concentrations of dissolved CO_2, as the low pH drives the inorganic carbon system towards the carbonic acid/carbon dioxide end of the equilibrium.

The very low nitrate concentrations in these wells suggest either denitrifying conditions in the aquifer, or that the surrounding lacustrine deposits limit infiltration of agriculturally impacted recharge. The presence of detectable ammonium, mildly negative to slightly positive ORP and the elevated concentrations of dissolved iron (several hundred to thousands of µg/L) and manganese (around 100 µg/L) all suggest mildly reducing conditions, within the nitrate/iron/manganese reduction field, but not achieving sulphate reduction.

6.4 Intermediate on-site borehole BHD, and off-site well G1

The high alkalinity, Na-HCO_3 nature of the groundwaters suggests a high degree of water-rock interaction. The combination of high alkalinity and pH appears to have suppressed calcium concentrations by the common ion effect at calcite saturation. Sodium can continue to accumulate in the water (> 400 mg/L) by a process of calcium removal by calcite precipitation and continued aluminosilicate hydrolysis, possibly complemented by cation exchange (Frengstad & Banks 2000, Banks & Frengstad 2006).

The modest chloride concentrations do not suggest any influence of deeper saline groundwaters.

Harder (1970) has shown that boron is readily substituted in illites and micas and is enriched in bituminous argillites such as the Kimmeridge Clay Formation, which possibly explains the elevated boron concentrations in the groundwater.

6.5 Deep (Corallian) on-site borehole BHE

In BHE, the elevated chloride concentrations indicate that the hydrochemical composition is influenced by a component of deep saline groundwater. The sodium excess over chloride, high alkalinity and very high pH suggests a further hydrochemical evolution under the influence of processes noted in BHD. The high pH and high alkalinity led to potential calcite oversaturation and the observed calcium concentrations of < 1 mg/L were due to removal of calcium by calcite precipitation. The removal of calcium by calcite precipitation also removes an important pH buffer in the groundwater system and allows the pH to evolve to high values and for sodium to continue to accumulate in the water (Frengstad & Banks 2000, Banks & Frengstad 2006).

575 The lack of sulphate suggests sulphate reducing conditions. The absence of iron and manganese
576 supports this interpretation, such metals having been removed from solution as sulphide mineral
577 phases. The concentrations of methane (> 40 mg/L) exceed its solubility in water (c. 31 mg/L at 10°C
578 and atmospheric pressure; corresponding to a Bunsen solubility coefficient of 0.0435 and density of
579 0.717 kg/m^3 at STP – Yamamoto et al. 1976, Air Liquide 2020) and account for the observed
580 effervescence during sampling. The low dissolved CO_2 content was simply due to the high pH, any free
581 carbonic acid having been converted to HCO_3^- or $CO_3^=$.

582

7. ORIGIN OF DISSOLVED METHANE AND CARBON DIOXIDE

7.1 Origin of Dissolved Methane and Ethane

The preindustrial mole fraction of methane in dry atmosphere was around 0.7 ppm (µmole/mole) but had reached a global average of 1.9 ppm by 2018 (Dlugokencky et al. 2011, 2020). Quay et al. (1999) cited the global average methane $\delta^{13}C$ as -47.2 to -47.7‰. Both the atmospheric methane content and its $\delta^{13}C$ vary depending on time of day and location (Bosquet et al. 2006, Stieger et al. (2019). An atmospheric content of 2 µmole $mole^{-1}$ and a methane solubility of 31 mg/L at 10°C would imply that one would expect an aqueous methane concentration of <0.1 µg/L for a water sample in equilibrium with the atmosphere.

The role of stable isotopes in identifying methane sources in the geo- and hydrosphere has long been recognised (Whiticar et al. 1986, Whiticar 1996). Bell et al. (2017) and Su et al. (2018) consider three different important sources of dissolved light alkanes in groundwater:

1. Thermogenesis. Thermogenesis is the main process responsible for producing commercial hydrocarbon reserves by the thermal degradation of more complex buried organic compounds, such as kerogen, commencing at around 70°C (Mahlstedt 2018). Methane is formed by the "cracking" of higher hydrocarbons and complex organics at elevated subsurface pressure and in a temperature window of 157 – 221°C (Stolper et al. 2014). The isotopic composition of thermogenic methane depends on the source rock (Schoell 1983, Whiticar 1996, Schloemer et al. 2016), but the $\delta^{13}C$ is typically relatively high, in the range -26 to -55‰ (Baldassare 2010). Thermogenic methane is also associated with higher hydrocarbons. For example, gas associated with oil deposits typically has an ethane and propane content of >5% (Schloemer et al. 2016).

2. Microbial methanogenesis by carboxylate fermentation pathways, e.g. of acetate (Jeris & McCarty 1965, Woltemate et al. 1984), to produce methane and carbon dioxide (sometimes termed acetoclastic methanogenesis; Schlesinger & Bernhardt 2013). Although this pathway does require anaerobic conditions, small quantities of methane can be produced in anaerobic micro-niches within otherwise relatively oxidising aquifers. This pathway is thought to be the source of low concentrations of methane in many of the UK's shallower aquifers.

$$CH_3COO^- + H_2O \rightarrow CH_4 + HCO_3^- \quad (1)$$

The $\delta^{13}C$ of methane generated by such processes is typically in the range -40 to -62‰ (Baldassare 2010) or -50 to -65‰ according to Whiticar et al. (1986) and Schloemer et al. (2016). Landfill and sewage gas methane, for example, has a typical $\delta^{13}C$ of -53 to -58‰ (Dlugokencky et al. 2011, Stieger et al. 2019).

615 3. Microbial methanogenesis involving reduction of carbon dioxide by hydrogen (or from formate as
616 a substrate), or hydrogenotrophic methanogenesis. The hydrogen is in turn derived from hydrogen-
617 producing acetogenic bacteria, breaking down more complex organic compounds such as higher fatty
618 acids (Angelidaki et al. 2011, Stevens et al. 2012). It requires a low redox potential, anaerobic
619 conditions and it is usual for sulphate reduction processes to have progressed to near completion.
620 Such conditions are typically found in organic-rich marine sediments, or deep, confined geological
621 strata.

622 $C_4H_7O_2^- + 2H_2O \rightarrow 2CH_3COO^- + H^+ + 2H_2$ (2)

623 $4H_2 + CO_2 \rightarrow 2H_2O + CH_4$ (3)

624 The $\delta^{13}C$ of methane generated by CO_2 reduction is typically very low, in the range -62 to -90‰
625 (Baldessare 2010) or -60 to -110‰ (Whiticar et al. 1986, Schloemer et al. 2016).

626 Subsurface bacterial oxidation of methane leads to a fractionation, leaving the residual methane
627 isotopically enriched in ^{13}C, relative to ^{12}C (Coleman et al. 1981) and this may be important in many
628 groundwater environments (Vigneron et al. 2017).

629 The boundary between microbial methane and thermogenic methane is often cited as around $\delta^{13}C$ =
630 -50‰ (Osborn & McIntosh 2010), although carboxylate fermentation pathways and microbial
631 oxidation may push microbiogenic dissolved methane into isotopically heavier territory. Where
632 isotopic evidence is ambiguous, the ratio of methane to heavier alkanes can be used as a diagnostic.
633 For both the bacterial methanogenetic pathways, ethane (and other higher hydrocarbon)
634 concentrations are typically low. The proportion of C_{2+} gases associated with biogenic methane is
635 usually <0.05% (Edwards & Durucan 1991), and the molar $C_1/(C_2+C_3)$ ratio is >1000 (Bernard et al.
636 1997). At least one study (Schloemer et al. 2016) has found low concentrations of ethane in relatively
637 shallow groundwaters in Saxony, Germany (ethane was above the detection limit of 20 nL/L in c. 25%
638 of the c. 1000 samples). It is suggested that the lowest molar $C_1/(C_2+C_3)$ ratio characteristic of biogenic
639 methane could be as low as 300 (Schloemer et al. 2016). A $C_1/(C_2+C_3)$ ratio of between 50 and 100 is
640 often cited as an upper limit for thermogenic methane (Bernard et al. 1976, Osborn & McIntosh 2010,
641 Vigneron et al. 2017).

642 Other geological processes for methane formation, such as methanol reduction (Jeris & McCarty 1965)
643 or abiotic methanogenesis, are considered implausible in this environment and will not be considered
644 further.

645 Finally, it should be remembered that shale gas and coal bed gas can be a combination of biogenic and
646 thermogenic components and may indeed lie on a continuum between the two (Golding et al. 2013).

Natural gas derived from the Bowland Shale or Zechstein Group horizons in the Kirby Misperton gas boreholes would be expected to be thermogenic, due to depth and temperature considerations. For example, shale gas from the Marcellus shale at depths of 866 m to 2.5 km in the Appalachians was characterised by a methane $\delta^{13}C$ of -27 to -42‰, well within the thermogenic range (Hakala 2014).

In the data set from the Kirby Misperton area, many of the groundwaters had a dissolved methane $\delta^{13}C$ of -48 to -50‰ (Figure 8). This is very similar to a typical atmospheric methane signature. It also falls in the groundwater methane range characteristic of acetate fermentation, but at the very lowest end of the range plausible for thermogenic methane. Thus, for samples where the methane concentration was consistently around the limit of quantification (<10 µg/L) and the dissolved methane $\delta^{13}C$ was c. -48 to -49‰ (Table 6), one can argue that the $\delta^{13}C$ either simply represents equilibration with atmospheric methane content, or could represent low concentrations of methane generated by freshwater acetate fermentation processes. For samples with median dissolved methane in the range 10-100 µg/L (S2, G2, G4, G5, G6, BHA, BHD), the dissolved methane median $\delta^{13}C$ was in the range -47 to -50‰. In this case, however, the dissolved methane concentrations were likely to be genuinely geogenic, rather than simply due to post-sampling atmospheric exchange, and the most likely source was acetate fermentation. A thermogenic source cannot be wholly ruled out although, if this were the case, one would expect to see a progressively stronger thermogenic signature with depth.

However, in the deepest samples (G3 and BHE), which have concentrations of dissolved methane >1 mg/L, the methane $\delta^{13}C$ shifts further into negative territory, more characteristic of methanogenesis by CO_2 reduction (median -59‰ and -71.9‰, respectively), with 25% of samples lower than -71.7‰ and -74.7‰, respectively. Microbial methanogenesis is typically restricted to temperatures <80°C and typically produces predominantly methane rather than other higher hydrocarbons (Mahlstedt 2018).

In borehole G1, which has a median dissolved methane concentration of 620 µg/L, most of the isotopic analyses returned methane $\delta^{13}C$ of -44‰ to -50‰, characteristic of acetate fermentation (or, conceivably, thermogenic) processes. However, 25% of the samples from G1 had a $\delta^{13}C$ of -65‰ or lower, placing them in the field of bacterial methanogenesis by CO_2 reduction. The temporal variability could be due to variable degree of re-equilibration with atmospheric air, although this was not observed clearly in samples from G3 or BHE. Alternatively, it could be due to the methane being derived from a mixture of sources – e.g. both acetate fermentation and CO_2 reduction, depending on redox conditions and substrate availability.

Identification of methane sources can be attempted by plotting the molar $C_1/(C_2+C_3)$ ratio versus methane $\delta^{13}C$ on a Bernard diagram (Bernard et al. 1976, 1977, Schloemer et al. 2016; Figure 9). For

borehole BHE, the very low $\delta^{13}C$ and $C_1/(C_2+C_3)$ ratio of 11000 - 14000 establish the methane as derived from bacterial methanogenesis by CO_2 reduction.

For G3, the $C_1/(C_2+C_3)$ ratio was much lower than BHE at 300 – 350. This is just at the lowermost range considered plausible for bacterial methanogenesis (Schloemer et al. 2016). The low $\delta^{13}C$ confirms bacterial methanogenesis as the main source of methane in G3, although the low $C_1/(C_2+C_3)$ ratio allows the possibility of the admixture of a component of thermogenic methane – indeed, the Kimmeridge Clay is known as a source rock for hydrocarbons and has reached sufficient maturity to have gas potential in some parts of East Yorkshire (Williams 1986, Gallois 2004). Alternatively, the methane may represent a bacteriogenic methane, subject to subsequent oxidation - a process that can increase $\delta^{13}C$ and decrease the methane/ethane ratio (Whiticar 1996, Ozgul 2002, Grassa et al. 2004).

In G1, the ethane concentration was consistently < 1µg/L, but median methane was c. 620 µg/L. This allows us to say that the $C_1/(C_2+C_3)$ ratio is in the bacterial methanogenesis field. The sporadically less negative $\delta^{13}C$ signature suggests that there may be components of acetate fermentation and CO_2 reduction.

For the other samples, the low methane concentrations (and absence of ethane) do not allow us to quantify the $C_1/(C_2+C_3)$ ratio or deduce anything from it.

7.2 Origin of Dissolved Carbon Dioxide

Marine carbonates typically form with a $\delta^{13}C$ of around 0‰, while atmospheric carbon dioxide has a typical $\delta^{13}C$ of −6 to −8‰ (Craig 1953, Cerling et al. 1991). This carbon dioxide is photosynthesised by plants, which are then decomposed by fungi and microbes. The resulting soil gas is enriched in CO_2 via respiration, and the bulk soil gas CO_2 resulting from C3 metabolic pathways (characteristic of temperate regions) typically has a $\delta^{13}C$ of − 27.5 to − 23‰ (Dörr & Münnich 1980, Cerling 1984, Alpers et al. 1990, Cerling et al. 1991, Clark & Fritz 1997, Bottrell et al. 2017).

When hydrochemically evolving groundwater in marine sedimentary rocks approaches equilibrium with calcite, the CO_2 ($\delta^{13}C$ = c. -26‰) is consumed by dissolution of marine calcite ($\delta^{13}C$ = -0‰), and the dissolved inorganic carbon (DIC, of which the dissolved CO_2 content is in dynamic equilibrium) is essentially a 1:1 mixture of the two components, with a $\delta^{13}C$ = c. -13‰.

As regards the ^{13}C signature of Kirby Misperton water samples, most of the groundwaters and the four surface waters typically show signatures of around -21 to -28‰, which suggests open systems, equilibrated with soil gas or biodegrading subsurface organic matter (Clark & Fritz 1997). The most hydrochemically "mature", deepest and highest pH water (with the lowest dissolved CO_2 content - BHE) has a far less

711 depleted ^{13}C signature (typically -7 to -15‰), which suggests closed system soil gas interaction with
712 limestone (carbonate) minerals. Indeed, a relatively high ^{13}C in DIC in methane-containing waters is
713 considered evidence (Golding et al. 2013) of bacterial methanogenesis by CO_2 reduction (preferential
714 enrichment of the residual DIC in ^{13}C).

715

8. DISCUSSION

The concept of documenting a "water quality baseline" for a potentially contaminating development site is an attractive idea. This, and other previous studies (Banks 2010), have demonstrated that it is somewhat more complex in practice, not only because groundwater quality can vary substantially laterally over short distances (contrast wells BHA-C with G2-G6 in this study), but also because it can be extremely dependent on depth. With increasing depth, groundwater can experience a steep increase in salinity and decrease in redox potential in a wide variety of geological environments. Over a 220 m depth interval at Kirby Misperton, the groundwater quality changes from a weakly acidic, sulphate-rich, Ca-HCO_3-SO_4 water to a brackish, highly reducing sodium chloride water with extremely high pH and alkalinity and a dissolved methane content of around 50 mg/L. In cases where the public is extremely sensitive to a commercial development (in this case, shale gas or hydraulic fracturing), it is essential that the natural background and its variability in three dimensions is clearly communicated.

Until recently, methane and other light hydrocarbons were not commonly analysed as dissolved components of UK groundwater. One of the earliest studies (Darling & Gooddy 2006) found that potable groundwaters from Mesozoic carbonate and sandstone aquifers exhibited ubiquitous low concentrations of dissolved methane; typically <10 µg/L, but with concentrations ranging up to 0.5 mg/L. Deeper Carboniferous and Triassic thermal or aquitard waters commonly contained higher concentrations (> 1.5 mg/L), with up to 16 mg/L being found in groundwater from Namurian shales in Lancashire. Darling & Gooddy (2006) found the highest dissolved methane concentrations were associated with elevated alkalinity and low concentrations of sulphate (both indicators of sulphate reduction).

Around the Kirby Misperton site, concentrations of dissolved methane ranged from up to c. 10 µg/L in shallow (c. 10 m depth, e.g., BHA) groundwaters, through a few tens to a few thousands of µg/L at intermediate depth (BHD, G1 and G3) to around 50 mg/L in the Corallian Oolite aquifer at 222 m depth (BHE). Low concentrations of dissolved methane, c. 10 µg/L, were even consistently detected in one of the surface water sampling sites (Costa Beck, S2). Dissolved ethane was regularly found (median 19 µg/L) in one of the off-site shallow well's groundwater (G3) and at lower concentrations (median 8 µg/L) in the on-site BHE's deep Corallian groundwater. In all cases, we believe that the dissolved light hydrocarbons detected were natural in origin. In the case of the shallower groundwaters, isotopic evidence suggests that the most likely origin was microbiological, probably via natural carboxylate fermentation pathways and possibly modified by microbial oxidation. In the deeper groundwaters, methanogenesis by carbon dioxide reduction under highly reducing conditions appears more likely.

748 In only one of the wells (G3) does the isotopic evidence and high ethane concentration suggest that
749 there may be a thermogenic component. This, in itself, does not imply a deep origin from the
750 commercial target reservoirs (the Zechstein Group carbonates or Carboniferous Bowland Shale), as
751 the possible thermogenic signature shows no sign of increasing with depth, and as the shallow
752 Kimmeridge Clay, which hosts well G3, is a known hydrocarbon source rock whose genetic history
753 suggests that it may contain thermogenic hydrocarbons. Alternatively, the signature could represent
754 oxidation of a microbial methane signature, with is accompanied by a relative enrichment in ^{13}C and
755 a depletion of methane relative to ethane (Whiticar 1996, Ozgul 2002, Grassa et al. 2004).

756 We thus conclude that the presence of dissolved methane is far from diagnostic of groundwater
757 contamination from hydrocarbon or hydrofracking operations. Rather, the study reported here and
758 the baseline studies of the British Geological Survey (Ward et al. 2018, 2020) suggest that dissolved
759 methane can be far more widespread in some specific shallow groundwater environments than
760 hitherto recognised. Furthermore, a possible thermogenic methane signature is not unequivocal
761 evidence of deep hydrocarbon contamination (Taherdangkoo et al. 2000), as near-surface subcrops of
762 low-permeability organic rich sediments, with a suitable diagenetic history, can potentially retain and
763 then release light hydrocarbons with a thermogenic signature, as previously noted by Bell et al. (2016).
764 A potential mixed thermogenic / bacteriogenic signature for shallow groundwater methane in the
765 region was also noted by Smedley et al. (2017), who postulated the Kimmeridge Clay Formation as
766 one possible source of this signature.

767 Specific sedimentary sequences can also release solutes to groundwater, whose presence might (in
768 the absence of background studies) be construed as evidence of contamination from hydrocarbon
769 operations. For example, the Kimmeridge Clay can release elevated concentrations of boron and
770 strontium to groundwater, even at relatively shallow depths.

771 The background hydrochemical study suggests that the main detrimental event to the water
772 environment during the period of the study (the Spring 2018 ammonium, potassium and iron pulse in
773 surface waters S1 and S4) may have been due to agricultural practices.

774

9. CONCLUSIONS

The monitoring of surface water and groundwater between April 2017 and September 2019 does not demonstrate any chemical impact on the hydrological environment due to operations in preparation for the hydraulic fracturing of the KM-8 shale gas well at the Kirby Misperton KMA wellsite. Because the monitoring only commenced following the drilling of the wells (KM-1, KM-3 and KM-8) on the KMA site, it can neither conclusively prove nor disprove an impact on the local hydrosphere. The 2017-2019 monitoring failed, however, to find any evidence of significant residual groundwater contamination either by hydrocarbon products, organic contaminants or saline formation waters which might have resulted from the drilling or operation of these wells. The proposed shale gas well (KM-8) was never hydraulically fractured. However, the data collected during this study could have formed a starting point to suggest baselines and trigger concentrations in connection with future hydraulic fracturing, using techniques suggested by Moutcoudiol et al. (2019) and others.

Monitoring has demonstrated that natural groundwater quality varies strongly with depth, from mildly acidic, Ca-HCO_3-SO_4 groundwaters in superficial / weathered Kimmeridge Clay strata within the bounds of KMA, to brackish, extremely high pH and alkalinity, highly reducing, Na-Cl waters at c. 220 m depth in the confined Corallian Oolite aquifer.

Shallow groundwater quality also varies laterally: at KMA, which lies on elevated terrain, devoid of the blanket of glaciolacustrine sediments laid down by the Pleistocene Lake Pickering, shallow groundwaters were mildly acidic and of Ca-HCO_3-SO_4 type. Only a short distance from KMA, where glaciolacustrine deposits overlie the Kimmeridge Clay Formation, shallow groundwaters typically have an alkaline pH, a high alkalinity, low calcium and have accumulated sodium in solution, well in excess of chloride. They were typically Na-HCO_3 waters.

This highlights the difficulties of establishing a water quality “baseline” in areas scheduled to be developed for hydrocarbon exploitation. Groundwater chemistry can vary sharply in both a lateral and a vertical direction; careful planning and a suitable 3-dimensional density of monitoring points is necessary to capture this variation.

Monitoring also highlighted the common occurrence of detectable dissolved methane (and occasionally, dissolved ethane) in natural groundwaters from different aquifers. The isotopic evidence also suggests that the methane was not derived from a single source but, rather, that there are multiple sources in the geological environment, within a relatively small area. The relatively modest concentrations of methane in shallow sediments in the KMA area are believed to be derived from carboxylate fermentative pathways in reducing micro-niches in the aquifer environment, as proposed

by Darling & Gooddy (2006). At greater depth, higher methane concentrations appear to be derived from bacterial methanogenesis via carbon dioxide reduction. In the deepest borehole BHE, to the Corallian Oolite Formation, concentrations of c. 50 mg/L dissolved methane were typically observed, higher than methane solubility at atmospheric pressure, leading to exsolution of methane during sampling.

In one, relatively shallow, offsite well (G3), the high concentration of dissolved ethane, relative to methane, suggested that the dissolved hydrocarbon content *may* have an admixture of a thermogenic signature. We postulate that this was not necessarily derived from deep Bowland Shale or Zechstein Group reservoirs – rather, it could be derived from traces of thermogenic hydrocarbons retained in the shallow, low permeability Kimmeridge Clay host aquifer, which has a diagenetic history compatible with thermogenesis of hydrocarbons. Thus, while a bacterial methanogenetic isotopic signature can usually be used to rule out derivation of dissolved methane from deep shale gas / hydrocarbon reservoirs, the presence of a possible thermogenic signature may not be sufficient in all geological environments to definitively prove a deep reservoir origin. In future studies, determination of the δ^2H of the methane, as well as the $\delta^{13}C$, would allow alternative diagnostic techniques for source identification – e.g. the Schoell (1980, 1988) diagram.

The findings of this study are broadly compatible to the British Geological Survey's broader baseline study of the Vale of Pickering (Smedley et al. 2017).

Rather good sample reproducibility for dissolved methane and ethane was achieved in this study, using a relatively simple sampling method (i.e., sampling water direct from pump discharge to a glass vial, with no headspace and immediately sealing and inverting). The method favoured by the British Geological Survey (BGS; flow-through sampling, with capture in a steel cylinder) exhibited poorer reproducibility in this particular study. Molofsky et al. (2016) noted especially poor reproducibility for sampling dissolved methane when effervescence was present. We note that the BGS method has been successfully used in other studies (Bell et al. 2016, 2017) and we speculate that the slow pumping rates (bladder pumps) coupled with visible methane exsolution and bubbles adhering to sample tubing, may explain the poor performance of the technique in this particular study. In future studies, the use of other innovative methods (e.g. IsoFlasks®; Molofsky et al. 2016) should be considered.

ACKNOWLEDGMENTS

Contains rainfall chemistry data supplied by Natural Environment Research Council under the Open Government Licence v3 (OGL).

We thank the British Geological Survey for providing the opportunity to carry out comparative study of dissolved methane sampling methodologies. We would also like to thank three anonymous reviewers for their insightful comments and suggestions.

FUNDING

The work described in this article was carried out by Envireau Water as a consultancy appointment to Third Energy. The University of Glasgow has partially supported DB's time input to the preparation of this paper.

REFERENCES

AHMAD, S.A., KHAN, M.H., HAQUE, M., 2018. Arsenic contamination in groundwater in Bangladesh: implications and challenges for healthcare policy. RMHP Volume 11, 251–261. https://doi.org/10.2147/RMHP.S153188

AIR LIQUIDE, 2020. Gas Encyclopedia. https://encyclopedia.airliquide.com/

ALI, W., RASOOL, A., JUNAID, M., ZHANG, H., 2019. A comprehensive review on current status, mechanism, and possible sources of arsenic contamination in groundwater: a global perspective with prominence of Pakistan scenario. Environ Geochem Health 41, 737–760. https://doi.org/10.1007/s10653-018-0169-x

ALLEN, D.J., BREWERTON, L.J., COLEBY, L.M., GIBBS, B.R., LEWIS, M.A., MACDONALD, A.M., WAGSTAFF, S.J., WILLIAMS, A.T., 1997. The physical properties of major aquifers in England and Wales. British Geological Survey Technical Report WD/97/34; Environment Agency R&D publication 8. British Geological Survey / Environment Agency, Keyworth, Nottinghamshire, UK.

AMBROSE, J., 2019. Fracking halted in England in major government U-turn. The Guardian. 2nd November 2019. https://www.theguardian.com/environment/2019/nov/02/fracking-banned-in-uk-as-government-makes-major-u-turn

ANGELIDAKI, I., KARAKASHEV, D., BATSTONE, D.J., PLUGGE, C.M., STAMS, A.J.M., 2011. Biomethanation and its potential, in: Methods in Enzymology. Elsevier, pp. 327–351. https://doi.org/10.1016/B978-0-12-385112-3.00016-0

BAIR, E.S., FREEMAN, D.C., SENKO, J.M., 2010. Expert panel technical report. Subsurface gas invasion. Bainbridge Township, Geauga County, Ohio. Ohio Department of Natural Resources, Columbus, Ohio, USA. https://oilandgas.ohiodnr.gov/portals/oilgas/pdf/bainbridge/DMRM%200%20Title%20Page,%20Preface,%20Acknowledgements.pdf

BALDASSARE, F.J., 2010. Applications in the use of isotope geochemistry to identify the origin of methane in the environment, in: Proceedings of the Groundwater Protection Council Annual Forum, September 27-29, 2010. Pennsylvania Department of Environmental Protection, Pittsburgh, Pennsylvania, USA. http://www.gwpc.org/sites/default/files/event-sessions/11Baldassare_Fred.pdf

BANKS, D., 1997. Hydrogeochemistry of Millstone Grit and Coal Measures groundwaters, south Yorkshire and north Derbyshire, UK. Quarterly Journal of Engineering Geology and Hydrogeology 30, 237–256. https://doi.org/10.1144/GSL.QJEG.1997.030.P3.06

BANKS, D., 2010. Chapter 1. Introduction, in: Reimann, C., Birke, M. (Eds.), Geochemistry of European Bottled Water. Borntraeger Science Publishers, Stuttgart, pp. 3–12.

BANKS, D., FRENGSTAD, B., 2006. Evolution of groundwater chemical composition by plagioclase hydrolysis in Norwegian anorthosites. Geochimica et Cosmochimica Acta 70, 1337–1355. https://doi.org/10.1016/j.gca.2005.11.025

BANKS, D., FRENGSTAD, B., MIDTGÅRD, A.K., KROG, J.R., STRAND, T., 1998. The chemistry of Norwegian groundwaters: I. The distribution of radon, major and minor elements in 1604 crystalline bedrock groundwaters. Science of The Total Environment 222, 71–91. https://doi.org/10.1016/S0048-9697(98)00291-5

BANKS, D., RØYSET, O., STRAND, T., SKARPHAGEN, H., 1995. Radioelement (U, Th, Rn) concentrations in Norwegian bedrock groundwaters. Environmental Geology 25, 165–180. https://doi.org/10.1007/BF00768546

BEARCOCK, J.M., SMEDLEY, P.L., MILNE, C.J., 2015. Baseline groundwater chemistry: the Corallian of the Vale of Pickering, Yorkshire (Groundwater Programme Open Report No. OR/15/048). British Geological Survey, Keyworth, Nottinghamshire, UK.

BELL, R.A., DARLING, W.G., MANAMSA, K., Ó DOCHARTAIGH, B.É., 2016. The baseline concentrations of methane in Great British groundwater - the national methane baseline survey (British Geological Survey No. OR/15/071). British Geological Survey, Keyworth, Nottinghamshire, UK.

BELL, R.A., DARLING, W.G., WARD, R.S., BASAVA-REDDI, L., HALWA, L., MANAMSA, K., Ó DOCHARTAIGH, B.E., 2017. A baseline survey of dissolved methane in aquifers of Great Britain. Science of The Total Environment 601–602, 1803–1813. https://doi.org/10.1016/j.scitotenv.2017.05.191

BERNARD, B.B., BROOKS, J.M., SACKETT, W.M., 1976. Natural gas seepage in the Gulf of Mexico. Earth and Planetary Science Letters 31, 48–54. https://doi.org/10.1016/0012-821X(76)90095-9

BERNARD, B., BROOKS, J.M., SACKETT, W.M., 1977. A geochemical model for characterization of hydrocarbon gas sources in marine sediments. Paper OTC 2934, in: Proc. 9th Annual Offshore Technology Conference, May 2-5, 1977. Houston, Texas, USA, pp. 435–438. https://doi.org/10.4043/2934-MS

BGS, 2000. Geological Survey of England and Wales 1:50,000 geological map series, sheet 53 Pickering (solid and drift).

BGS, 2020. British Geological Survey lexicon of named rock units - Kimmeridge Clay Formation [WWW Document]. URL https://webapps.bgs.ac.uk/lexicon/lexicon.cfm?pub=KC (accessed 10.31.20).

BOTTRELL, S., HIPKINS, E.V., LANE, J.M., ZEGOS, R.A., BANKS, D., FRENGSTAD, B.S., 2019. Carbon-13 in groundwater from English and Norwegian crystalline rock aquifers: a tool for deducing the origin of alkalinity? Sustain. Water Resour. Manag. 5, 267–287. https://doi.org/10.1007/s40899-017-0203-7

BOUSQUET, P., CIAIS, P., MILLER, J.B., DLUGOKENCKY, E.J., HAUGLUSTAINE, D.A., PRIGENT, C., VAN DER WERF, G.R., PEYLIN, P., BRUNKE, E.-G., CAROUGE, C., LANGENFELDS, R.L., LATHIÈRE, J., PAPA, F., RAMONET, M., SCHMIDT, M., STEELE, L.P., TYLER, S.C., WHITE, J., 2006. Contribution of anthropogenic and natural sources to atmospheric methane variability. Nature 443, 439–443. https://doi.org/10.1038/nature05132

CAPE, J.N., SMITH, R.I., LEAVER, D.S., 2014. Cleaned UK rainfall chemistry data (1986-2011). NERC Environmental Information Data Centre. (Dataset). https://doi.org/10.5285/ada39609-ddec-4cbe-85c2-4fdd6bd774d7

CATALYST, 2016. Quantitative support for EPA's finding of no widespread, systemic effects to drinking water resources from hydraulic fracturing. Report by Catalyst Environmental Solutions for American Petroleum

913 Institute. July 2016. https://www.api.org/-/media/Files/Oil-and-Natural-Gas/Hydraulic-Fracturing/API-
914 Support-for-No-Widespread-Effects-Finding.pdf

915 CERLING, T.E., 1984. The stable isotopic composition of modern soil carbonate and its relationship to climate.
916 Earth and Planetary Science Letters 71, 229–240. https://doi.org/10.1016/0012-821X(84)90089-X

917 CERLING, T.E., SOLOMON, D.K., QUADE, J., BOWMAN, J.R., 1991. On the isotopic composition of carbon in soil carbon
918 dioxide. Geochimica et Cosmochimica Acta, The Macalpine Hills Lunar Meteorite Consortium 55, 3403–3405.
919 https://doi.org/10.1016/0016-7037(91)90498-T

920 CLARK, I.D., FRITZ, P., 1997. Environmental isotopes in hydrogeology. CRC Press/Lewis Publishers, Boca Raton, FL.

921 COLEMAN, D.D., RISATTI, J.B., SCHOELL, M., 1981. Fractionation of carbon and hydrogen isotopes by methane-
922 oxidizing bacteria. Geochimica et Cosmochimica Acta 45, 1033–1037. https://doi.org/10.1016/0016-
923 7037(81)90129-0

924 COPE, J.C.W., 1974. New information on the Kimmeridge Clay of Yorkshire. Proceedings of the Geologists'
925 Association 85, 211–221. https://doi.org/10.1016/S0016-7878(74)80024-6

926 CRAIG, H., 1953. The geochemistry of the stable carbon isotopes. Geochimica et Cosmochimica Acta 3, 53–92.
927 https://doi.org/10.1016/0016-7037(53)90001-5

928 DARLING, W.G., GOODDY, D.C., 2006. The hydrogeochemistry of methane: Evidence from English groundwaters.
929 Chemical Geology 229, 293–312. https://doi.org/10.1016/j.chemgeo.2005.11.003

930 DARRAH, T.H., VENGOSH, A., JACKSON, R.B., WARNER, N.R., POREDA, R.J., 2014. Noble gases identify the mechanisms of
931 fugitive gas contamination in drinking-water wells overlying the Marcellus and Barnett Shales. Proc Natl Acad
932 Sci USA 111, 14076–14081. https://doi.org/10.1073/pnas.1322107111

933 DLUGOKENCKY, E.J., CROTWELL, A.M., THONING, K.W., MUND, J.W., 2019. Atmospheric methane from quasi-continuous
934 measurements at Barrow, Alaska and Mauna Loa, Hawaii, 1986-2019, Version: 2020-03.
935 https://doi.org/10.15138/VE0C-BE70

936 DLUGOKENCKY, E.J., NISBET, E.G., FISHER, R., LOWRY, D., 2011. Global atmospheric methane: budget, changes and
937 dangers. Phil. Trans. R. Soc. A. 369, 2058–2072. https://doi.org/10.1098/rsta.2010.0341

938 DÖRR, H., MÜNNICH, K.O., 1980. Carbon-14 and Carbon-13 in Soil Co2. Radiocarbon 22, 909–918.
939 https://doi.org/10.1017/S0033822200010316

940 EDWARDS, J.S., DURUCAN, S., 1991. The origins of methane. Mining Science and Technology 12, 193–204.
941 https://doi.org/10.1016/0167-9031(91)91686-C

942 ENVIREAU WATER, 2017A. KM8 monitoring boreholes; as-built construction report. KM8 well, Kirby Misperton A
943 wellsite, North Yorkshire. REV04. Envireau Water, Richmond, North Yorkshire, UK.
944 https://consult.environment-agency.gov.uk/onshore-oil-and-gas/third-energy-kirby-misperton-
945 information-

page/supporting_documents/PreOp%204%20%20Borehole%20Construction%20Report%20r4%20revised%20Sept%2017.pdf

ENVIREAU WATER, 2017B. Baseline water quality data, April-June 2017. Kirby Misperton A wellsite, North Yorkshire. Envireau Water, Richmond, North Yorkshire, September 2017. https://consult.environment-agency.gov.uk/onshore-oil-and-gas/third-energy-kirby-misperton-information-page/supporting_documents/KMA%20Baseline%20Water%20Quality%20Data_April%20to%20June%202017_Redacted.pdf

ENVIRONMENT AGENCY, 2016. Kirby Misperton A wellsite. Permit number EPR/DB3002HE. https://consult.environment-agency.gov.uk/onshore-oil-and-gas/third-energy-kirby-misperton-information-page/supporting_documents/Waste%20Permit.pdf

ENVIRONMENT AGENCY, 2017. Kirby Misperton A wellsite. Methane survey. May 2017. https://consult.environment-agency.gov.uk/onshore-oil-and-gas/third-energy-kirby-misperton-information-page/supporting_documents/EA%20Methane%20Monitoring%20KM8%20%20CH4%20Plots%20%20170518.pdf

ENVIRONMENT AGENCY, 2020. Third Energy - Kirby Misperton (KM8 well) information page - Environment Agency. Opened 1 Jun 2017; closed 31 May 2020 [WWW Document]. URL https://consult.environment-agency.gov.uk/onshore-oil-and-gas/third-energy-kirby-misperton-information-page/ (accessed 4.10.21).

EVANS, D.J.A., BATEMAN, M.D., ROBERTS, D.H., MEDIALDEA, A., HAYES, L., DULLER, G.A.T., FABEL, D., CLARK, C.D., 2017. Glacial Lake Pickering: stratigraphy and chronology of a proglacial lake dammed by the North Sea Lobe of the British–Irish Ice Sheet. Journal of Quaternary Science 32, 295–310. https://doi.org/10.1002/jqs.2833

FORD, J.R., HUGHES, L., BURKE, H.F., LEE, J.R., 2015. The Vale of Pickering: an initial summary of the Quaternary/superficial geology and data holdings (Geology & Regional Geophysics Programme Open Report No. OR/15/064). British Geological Survey, Keyworth, Nottinghamshire, UK.

FRENGSTAD, B., BANKS, D., 2000. Evolution of high-pH Na-HCO3 groundwaters in anorthosites: silicate weathering or cation exchange? in: Sililo et al. (Eds) “Groundwater: Past Achievements and Future Challenges”, Proc. XXXIInd Congress of the International Association of Hydrogeologists, Cape Town, South Africa. Balkema, Rotterdam, Netherlands, pp. 493–498.

FRENGSTAD, B., MIDTGÅRD SKREDE, A.K., BANKS, D., KROG, J.R., SIEWERS, U., 2000. The chemistry of Norwegian groundwaters: III. The distribution of trace elements in 476 crystalline bedrock groundwaters, as analysed by ICP-MS techniques. Science of The Total Environment 246, 21–40. https://doi.org/10.1016/S0048-9697(99)00413-1

GALLOIS, R.W., 2004. The Kimmeridge Clay: the most intensively studied formation in Britain. Open University Geological Journal 25, 33–38.

GOLDING, S.D., BOREHAM, C.J., ESTERLE, J.S., 2013. Stable isotope geochemistry of coal bed and shale gas and related production waters: A review. International Journal of Coal Geology 120, 24–40. https://doi.org/10.1016/j.coal.2013.09.001

GOLDING, S.D., BOREHAM, C.J., ESTERLE, J.S., 2013. Stable isotope geochemistry of coal bed and shale gas and related production waters: A review. International Journal of Coal Geology 120, 24–40. https://doi.org/10.1016/j.coal.2013.09.001

GOODDY, D.C., DARLING, W.G., 2005. The potential for methane emissions from groundwaters of the UK. Science of The Total Environment 339, 117–126. https://doi.org/10.1016/j.scitotenv.2004.07.019

GRANATO, G.E., DESIMONE, L.A., BARBARO, J.R., JEZNACH, L.C., 2015. Methods for evaluating potential sources of chloride in surface waters and groundwaters of the conterminous United States: U.S. Geological Survey Open-File Report 2015–1080, 89 pp. http://dx.doi.org/10.3133/ofr20151080

GRASSA, F., CAPASSO, G., FAVARA, R., INGUAGGIATO, S., FABER, E., VALENZA, M., 2004. Molecular and isotopic composition of free hydrocarbon gases from Sicily, Italy. Geophysical Research Letters 31. https://doi.org/10.1029/2003GL019362

HAARHOFF, M., HARRISON, D., HUGHES, F., TAYLOR, C., PEARSON, A., EMMS, G., MORTIMER, A., 2016. The history of exploration and development of gas fields in North Yorkshire, in: Abstracts of the European Oil and Gas Industry History Conference; 3-4 March 2016, London. Geological Society of London, London, UK, pp. 24–26. https://cms.geolsoc.org.uk/~/media/shared/documents/groups/specialist/energy/Oil%20History%20Abstract%20Book.pdf?la=en

HAARHOFF, M.Q., HUGHES, F., HEATH-CLARKE, M., HARRISON, D., TAYLOR, C., WARE, D.L., EMMS, G.G., MORTIMER, A., 2018. The history of hydrocarbon exploration and development in North Yorkshire. Geological Society, London, Special Publications 465, 119–136. https://doi.org/10.1144/SP465.12

HAKALA, J.A., 2014. Use of stable isotopes to identify sources of methane in Appalachian Basin shallow groundwaters: a review. Environ. Sci.: Processes Impacts 16, 2080–2086. https://doi.org/10.1039/C4EM00140K

HARDER, H., 1970. Boron content of sediments as a tool in facies analysis. Sedimentary Geology 4, 153–175. https://doi.org/10.1016/0037-0738(70)90009-6

HOOD, C., STIDWORTHY, A., WARD, R., SMEDLEY, P., CAVE, M., 2017. Preparation of statistically formulated baselines using existing data at an onshore oil and gas site (Kirby Misperton in Yorkshire) (No. FM1159/R2/17). Cambridge Environmental Research Consultants, Cambridge, UK.

JACKSON, R.B., VENGOSH, A., DARRAH, T.H., WARNER, N.R., DOWN, A., POREDA, R.J., OSBORN, S.G., ZHAO, K., KARR, J.D., 2013. Increased stray gas abundance in a subset of drinking water wells near Marcellus shale gas extraction. Proceedings of the National Academy of Sciences 110, 11250–11255. https://doi.org/10.1073/pnas.1221635110

1014 JACKSON, R.E., GORODY, A.W., MAYER, B., ROY, J.W., RYAN, M.C., STEMPVOORT, D.R.V., 2013. Groundwater protection
1015 and unconventional gas extraction: The critical need for field-based hydrogeological research. Groundwater
1016 51, 488–510. https://doi.org/10.1111/gwat.12074

1017 JERIS, J.S., MCCARTY, P.L., 1965. The biochemistry of methane fermentation using C14 tracers. Journal (Water
1018 Pollution Control Federation) 37, 178–192. www.jstor.org/stable/25035234

1019 LINCOLN, P., EDDEY, L., MATTHEWS, I., PALMER, A., BATEMAN, M., 2017. The Quaternary of the Vale of Pickering: Field
1020 Guide [WWW Document]. URL https://www.nhbs.com/the-quaternary-of-the-vale-of-pickering-book
1021 (accessed 4.10.21).

1022 MAHLSTEDT, N., 2018. Thermogenic Formation of Hydrocarbons in Sedimentary Basins, in: Wilkes, H. (Ed.),
1023 Hydrocarbons, Oils and Lipids: Diversity, Origin, Chemistry and Fate, Handbook of Hydrocarbon and Lipid
1024 Microbiology. Springer International Publishing, Cham, pp. 1–30. https://doi.org/10.1007/978-3-319-54529-
1025 5_15-1

1026 MAIR, R., BICKLE, M., GOODMAN, D., KOPPELMAN, B., ROBERTS, J., SELLEY, R., SHIPTON, Z., THOMAS, H., WALKER, A., WOODS,
1027 E., YOUNGER, P.L., 2012. Shale gas extraction in the UK: a review of hydraulic fracturing. Royal Society and
1028 Royal Academy of Engineering, London, UK. https://www.raeng.org.uk/publications/reports/shale-gas-
1029 extraction-in-the-uk

1030 MIDDLETON, D.R.S., WATTS, M.J., HAMILTON, E.M., FLETCHER, T., LEONARDI, G.S., CLOSE, R.M., EXLEY, K.S., CRABBE, H.,
1031 POLYA, D.A., 2016. Prolonged exposure to arsenic in UK private water supplies: toenail, hair and drinking water
1032 concentrations. Environ. Sci.: Processes Impacts 18, 562–574. https://doi.org/10.1039/C6EM00072J

1033 MOLOFSKY, L.J., RICHARDSON, S.D., GORODY, A.W., BALDASSARE, F., BLACK, J.A., MCHUGH, T.E., CONNOR, J.A. 2016. Effect
1034 of different sampling methodologies on measured methane concentrations in groundwater samples. Ground
1035 Water 54(5), 669-680. https://doi.org/10.1111/gwat.12415

1036 MONTCOUDIOL, N., BANKS, D., ISHERWOOD, C., GUNNING, A., BURNSIDE, N., 2019. Baseline groundwater monitoring for
1037 shale gas extraction: definition of baseline conditions and recommendations from a real site (Wysin,
1038 Northern Poland). Acta Geophys. 67, 365–384. https://doi.org/10.1007/s11600-019-00254-w

1039 OSBORN, S.G., MCINTOSH, J.C., 2010. Chemical and isotopic tracers of the contribution of microbial gas in Devonian
1040 organic-rich shales and reservoir sandstones, northern Appalachian Basin. Applied Geochemistry 25 (3), 456-
1041 471. https://doi.org/10.1016/j.apgeochem.2010.01.001

1042 OSBORN, S.G., VENGOSH, A., WARNER, N.R., JACKSON, R.B., 2011. Methane contamination of drinking water
1043 accompanying gas-well drilling and hydraulic fracturing. Proceedings of the National Academy of Sciences
1044 108, 8172–8176. https://doi.org/10.1073/pnas.1100682108

1045 OZGUL, E., 2002. Geochemical assessment of gaseous hydrocarbons: mixing of bacterial and thermogenic
1046 methane in the deep subsurface petroleum system. Gulf of Mexico continental slope (MSc dissertation).
1047 Texas A & M University, College Station, Texas, USA.

https://oaktrust.library.tamu.edu/bitstream/handle/1969.1/223/etd-07182002-124338-1.pdf?sequence=1&isAllowed=y

POWELL, J.H., FORD, J.R., RIDING, J.B., 2016. Diamicton from the Vale of Pickering and Tabular Hills, north-east Yorkshire: evidence for a Middle Pleistocene (MIS 8) glaciation? Proceedings of the Geologists' Association 127, 575–594. https://doi.org/10.1016/j.pgeola.2016.09.002

QUAY, P., STUTSMAN, J., WILBUR, D., SNOVER, A., DLUGOKENCKY, E., BROWN, T., 1999. The isotopic composition of atmospheric methane. Global Biogeochem. Cycles 13, 445–461. https://doi.org/10.1029/1998GB900006

REEVES, M.J., PARRY, E.L., RICHARDSON, G., 1978. Preliminary evaluation of the groundwater resources of the western part of the Vale of Pickering. Quarterly Journal of Engineering Geology and Hydrogeology 11, 253–262. https://doi.org/10.1144/GSL.QJEG.1978.011.03.05

REIMANN, C., FILZMOSER, P., 2000. Normal and lognormal data distribution in geochemistry: death of a myth. Consequences for the statistical treatment of geochemical and environmental data. Environmental Geology 39, 1001-1014. https://doi.org/10.1007/s002549900081

RIVETT, M.O., BUSS, S.R., MORGAN, P., SMITH, J.W.N., BEMMENT, C.D., 2008. Nitrate attenuation in groundwater: a review of biogeochemical controlling processes. Water Research 42 (16), 4215-4232. https://doi.org/10.1016/j.watres.2008.07.020

RIVETT, M.O., CUTHBERT, M.O., GAMBLE, R., CONNON, L.E., PEARSON, A., SHEPLEY, M.G., DAVIS, J., 2016. Highway deicing salt dynamic runoff to surface water and subsequent infiltration to groundwater during severe UK winters. Science of The Total Environment 565, 324-338. https://doi.org/10.1016/j.scitotenv.2016.04.095

ROBERTS, H.M., SHILLER, A.M., 2015. Determination of dissolved methane in natural waters using headspace analysis with cavity ring-down spectroscopy. Analytica Chimica Acta 856, 68–73. https://doi.org/10.1016/j.aca.2014.10.058

SCHLESINGER, W.H., BERNHARDT, E.S., 2013. Chapter 7 - Wetland ecosystems. In: Schlesinger, W.S. & Bernhardt, E.S. (eds) "Biogeochemistry", 3rd edition, 233-274. Academic Press. https://doi.org/10.1016/B978-0-12-385874-0.00007-8

SCHLOEMER, S., ELBRACHT, J., BLUMENBERG, M., ILLING, C.J., 2016. Distribution and origin of dissolved methane, ethane and propane in shallow groundwater of Lower Saxony, Germany. Applied Geochemistry 67, 118–132. https://doi.org/10.1016/j.apgeochem.2016.02.005

SCHOELL, M., 1980. The hydrogen and carbon isotopic composition of methane from natural gases of various origins. Geochimica et Cosmochimica Acta 44, 649–661. https://doi.org/10.1016/0016-7037(80)90155-6

SCHOELL, M., 1983. Genetic characterization of natural gases. AAPG Bulletin 67. https://doi.org/10.1306/AD46094A-16F7-11D7-8645000102C1865D

SCHOELL, M., 1988. Multiple origins of methane in the Earth. Chemical Geology, Origins of Methane in the Earth 71, 1–10. https://doi.org/10.1016/0009-2541(88)90101-5

1082 SHAND, P., TYLER-WHITTLE, R., MORTON, M., SIMPSON, E., LAWRENCE, A.R., PACEY, J., HARGREAVES, R., 2002. Baseline
1083 report series 1: The Permo-Triassic sandstones of the Vale of York (Groundwater Systems and Water Quality
1084 Programme No. CR/02/102N). British Geological Survey & Environment Agency, Keyworth, Nottinghamshire,
1085 UK & Solihull, UK.

1086 SHANKAR, S., SHANKER, U., SHIKHA, 2014. Arsenic contamination of groundwater: a review of sources, prevalence,
1087 health risks, and strategies for mitigation. The Scientific World Journal 2014, e304524.
1088 https://doi.org/10.1155/2014/304524

1089 SHEER, 2018. Deliverable 8.2. Guidelines for the monitoring of shale gas exploration and exploitation induced
1090 environmental impacts. Shale gas exploration and exploitation induced risks (SHEER). EU Horizon 2020
1091 project grant agreement 640896. http://www.sheerproject.eu/images/deliverables/SHEER-Deliverable-
1092 8.2.pdf

1093 SMEDLEY, P.L., WARD, R.S., BEARCOCK, J.M., BOWES, M.J., 2017. Establishing the baseline in groundwater chemistry
1094 in connection with shale-gas exploration: Vale of Pickering, UK. Procedia Earth and Planetary Science, 15th
1095 Water-Rock Interaction International Symposium, WRI-15 17, 678–681.
1096 https://doi.org/10.1016/j.proeps.2016.12.143

1097 STEVENS, S.H., FERRY, J.G., SCHOELL, M., 2012. Methanogenic conversion of CO2 into CH4: a potential remediation
1098 technology for geologic CO2 storage sites. US Department of Energy, Chicago, USA.
1099 https://www.osti.gov/servlets/purl/1041046/

1100 STIEGER, J., BAMBERGER, I., SIEGWOLF, R.T.W., BUCHMANN, N., EUGSTER, W., 2019. Source partitioning of atmospheric
1101 methane using stable carbon isotope measurements in the Reuss Valley, Switzerland. Isotopes in
1102 Environmental and Health Studies 55, 1–24. https://doi.org/10.1080/10256016.2018.1561448

1103 STOLPER, D.A., LAWSON, M., DAVIS, C.L., FERREIRA, A.A., NETO, E.V.S., ELLIS, G.S., LEWAN, M.D., MARTINI, A.M., TANG, Y.,
1104 SCHOELL, M., SESSIONS, A.L., EILER, J.M., 2014. Formation temperatures of thermogenic and biogenic methane.
1105 Science 344, 1500–1503. https://doi.org/10.1126/science.1254509

1106 STRIGGOW, B., 2013. Field measurement of oxidation-reduction potential (ORP). United States Environmental
1107 Protection Agency operating procedure SESDPROC-113-R1, Athens, Georgia.

1108 SU, X., ZHAO, W., XIA, D., 2018. The diversity of hydrogen-producing bacteria and methanogens within an in situ
1109 coal seam. Biotechnol Biofuels 11, 245. https://doi.org/10.1186/s13068-018-1237-2

1110 TAHERDANGKOO, R., TATOMIR, A., SAUTER, M., 2020. Modeling of methane migration from gas wellbores into shallow
1111 groundwater at basin scale. Environ Earth Sci 79, Article 432. https://doi.org/10.1007/s12665-020-09170-5

1112 TEASDALE, C.J., HALL, J.A., MARTIN, J.P., MANNING, D.A.C., 2019. Discriminating methane sources in ground gas
1113 emissions in NW England. Quarterly Journal of Engineering Geology and Hydrogeology 52, 110–122.
1114 https://doi.org/10.1144/qjegh2018-083

1115 THIRD ENERGY, 2017A. Hydraulic fracture plan for Well KM-8. Kirby Misperton, Alpha wellsite. Third Energy.
1116 September 2017. https://consult.environment-agency.gov.uk/onshore-oil-and-gas/third-energy-kirby-
1117 misperton-information-page/user_uploads/pre-op-2-hydraulic-fracture-plan-sept-17.pdf

1118 THIRD ENERGY, 2017B. Kirby Misperton A wellsite; KM8 production well; hydraulic fracture stimulation –
1119 environmental monitoring plan. Revision 8 Third Energy report TE-EPRA-KM8-HFS-EMP-10. 5th October 2017.
1120 https://consult.environment-agency.gov.uk/onshore-oil-and-gas/third-energy-kirby-misperton-
1121 information-page/user_uploads/pre-op-3-emissions-monitoring-plan-2.pdf

1122 TRIBOVILLARD, N.-P., DESPRAIRIES, A., LALLIER-VERGÈS, E., BERTRAND, P., MOUREAU, N., RAMDANI, A., RAMANAMPISOA, L.,
1123 1994. Geochemical study of organic-matter rich cycles from the Kimmeridge Clay Formation of Yorkshire
1124 (UK): productivity versus anoxia. Palaeogeography, Palaeoclimatology, Palaeoecology 108, 165–181.
1125 https://doi.org/10.1016/0031-0182(94)90028-0

1126 U.S.EPA, 2015. Retrospective case study in Killdeer, North Dakota - Study of the potential impacts of hydraulic
1127 fracturing on drinking water resources (No. EPA 600/R-14/103). Washington, DC, USA.

1128 U.S.EPA, 2016. Hydraulic fracturing for oil and gas: impacts from the hydraulic fracturing water cycle on drinking
1129 water resources in the United States (final report) (No. EPA/600/R-16/236F). U.S. Environmental Protection
1130 Agency, Washington, DC, USA. https://cfpub.epa.gov/ncea/hfstudy/recordisplay.cfm?deid=332990

1131 U.S.EPA, 2017. Response to the U.S. Environmental Protection Agency's Science Advisory Board Review of the
1132 draft report: Assessment of the potential impacts of hydraulic fracturing for oil and gas on drinking water
1133 resources. January 2017. U.S. Environmental Protection Agency, Washington, DC, USA.
1134 https://ofmpub.epa.gov/eims/eimscomm.getfile?p_download_id=530129

1135 UK GOVERNMENT, 2019. Press release: government end support for fracking.
1136 https://www.gov.uk/government/news/government-ends-support-for-fracking

1137 VENGOSH, A., WARNER, N., JACKSON, R., DARRAH, T., 2013. The effects of shale gas exploration and hydraulic fracturing
1138 on the quality of water resources in the United States. Procedia Earth and Planetary Science 7, 863–866.
1139 https://doi.org/10.1016/j.proeps.2013.03.213

1140 VIDIC, R.D., BRANTLEY, S.L., VANDENBOSSCHE, J.M., YOXTHEIMER, D., ABAD, J.D., 2013. Impact of shale gas development
1141 on regional water quality. Science 340. https://doi.org/10.1126/science.1235009

1142 VIGNERON, A., BISHOP, A., ALSOP, E. B., HULL, K., RHODES, I., HENDRICKS, R., HEAD, I. M., TSESMETZIS, N., 2017. Microbial
1143 and isotopic evidence for methane cycling in hydrocarbon-containing groundwater from the Pennsylvania
1144 Region. Frontiers in Microbiology 8, 593. https://doi.org/10.3389/fmicb.2017.00593

1145 WARD, R.S., SMEDLEY, P.L., ALLEN, G., BAPTIE, B.J., CAVE, M.R., DARAKTCHIEVA, Z., FISHER, R., HAWTHORN, D., JONES,
1146 D.G., LEWIS, A., LOWRY, D., LUCKETT, R., MARCHANT, B.P., PURVIS, R.M., WILDE, S., 2018. *Environmental baseline*
1147 *monitoring : Phase III final report (2017-2018).* British Geological Survey report OR/18/026, Nottingham, UK,
1148 143pp. http://nora.nerc.ac.uk/id/eprint/521380/

1149 WARD, R.S., SMEDLEY, P.L., ALLEN, G., BAPTIE, B.J., BARKER, P., BARKWITH, A.K.A.P., BATES, P., BATESON, L., BELL, R.A.,
1150 COLEMAN, M., CREMEN, G., CREWDSON, E., DARAKTCHIEVA, Z., GONG, M., HOWARTH, C.H., FRANCE, J., LEWIS, A.C., LISTER,
1151 T.R., LOWRY, D., LUCKETT, R., MALLIN MARTIN, D., MARCHANT, B.P., MILLER, C.A., MILNE, C.J., NOVELLINO, A., PITT, J.,
1152 PURVIS, R.M., RIVETT, M.O., SHAW, J., TAYLOR-CURRAN, H., WASIEKIEWICZ, J.M., WERNER, M., WILDE, S.,
1153 2020. *Environmental monitoring : phase 5 final report (April 2019 - March 2020).* British Geological Survey
1154 report OR/20/035, Nottingham, UK, 137pp. http://nora.nerc.ac.uk/id/eprint/528719/

1155

1156 WARNER, N.R., KRESSE, T.M., HAYS, P.D., DOWN, A., KARR, J.D., JACKSON, R.B., VENGOSH, A., 2013. Geochemical and
1157 isotopic variations in shallow groundwater in areas of the Fayetteville Shale development, north-central
1158 Arkansas. Applied Geochemistry 35, 207–220. https://doi.org/10.1016/j.apgeochem.2013.04.013

1159 WHITICAR, M.J., FABER, E., SCHOELL, M., 1986. Biogenic methane formation in marine and freshwater environments:
1160 CO2 reduction vs. acetate fermentation—Isotope evidence. Geochimica et Cosmochimica Acta 50, 693–709.
1161 https://doi.org/10.1016/0016-7037(86)90346-7

1162 WHITICAR, M.J., 1996. Stable isotope geochemistry of coals, humic kerogens and related natural gases.
1163 International Journal of Coal Geology 32, 191–215. https://doi.org/10.1016/S0166-5162(96)00042-0

1164 WILLIAMS, P.F.V., 1986. Petroleum geochemistry of the Kimmeridge Clay of onshore Southern and Eastern
1165 England. Marine and Petroleum Geology 3, 258–281. https://doi.org/10.1016/0264-8172(86)90032-2

1166 WOLTEMATE, I., WHITICAR, M.J., SCHOELL, M., 1984. Carbon and hydrogen isotopic composition of bacterial methane
1167 in a shallow freshwater lake: Isotopes of bacterial methane. Limnol. Oceanogr. 29, 985–992.
1168 https://doi.org/10.4319/lo.1984.29.5.0985

1169 YAMAMOTO, S., ALCAUSKAS, J.B., CROZIER, T.E., 1976. Solubility of methane in distilled water and seawater. J. Chem.
1170 Eng. Data 21, 78–80. https://doi.org/10.1021/je60068a029

1171

1172 **Table 1 Listing of monitored analytical parameters.** Analytical methods for parameters discussed in
1173 this paper are documented in Section 4.1. For other parameters, analytical methods and results can
1174 be found via the Environment Agency (2020) web page and in Envireau Water (2017b).

No	Parameter	No	Parameter
	General Inventory:	**33**	Nickel
1	Methane	**34**	Nitrate as NO3
2	Acrylamide	**35**	Nitrite as NO2
3	Alkalinity as CaCO3	**36**	Oxygen Reduction Potential
4	Ammoniacal Nitrogen as N	**37**	pH
5	Arsenic	**38**	Potassium
6	Aluminium	**39**	Salinity
7	Antimony	**40**	Selenium
8	Barium	**41**	Silver
9	Beryllium	**42**	Sodium
10	BOD (settled)	**43**	Strontium
11	Boron	**44**	Total petroleum hydrocarbons (including Benzene, diesel range organics (nC10 to nC24), gasoline range organics (nC5 to nC10), m/p Xylenes, o Xylene, MTBE, Toluene, Xylene, Ethylbenzene)
12	Bromide	**45**	Total Dissolved Solids
13	δ13C-CH4	**46**	Total Suspended Solids
14	δ13C-CO2	**47**	Vanadium
15	Cadmium	**48**	Zinc
16	Calcium		
17	Carbon Dioxide		***Fracture fluid additives:***
18	Chloride	**49**	Acetic acid;
19	Chromium (total)	**50**	Sodium persulphate;
20	Cobalt		
21	COD (Settled)		***Other chemical inventory:***
22	Copper	**51**	Formaldehyde;
23	Dissolved Butane	**52**	Ethylene glycol;
24	Dissolved Propane		
25	Dissolved Ethane		***Indicators of Fracture Fluid additives:***
26	Dissolved Methane	**53**	Sulphate
27	Fluoride	**54**	Bicarbonate alkalinity
28	Iron (total)	**55**	Anionic surfactants
29	Lead	**56**	Non-ionic surfactants
30	Lithium		
31	Magnesium		
32	Mercury		

1175

1176 **Table 2. Characteristics of the five on-site (BHA-BHE) and six off-site monitoring wells (G1-G6).** Asl =
1177 above sea level. Bgl = below ground level. SUP/WKC = Quaternary superficial materials and/or
1178 weathered Kimmeridge Clay; KC = unweathered Kimmeridge Clay. Open interval = interval straddled
1179 by well screen (BHA to BHD) or open section (BHE). Locations of G1-G6 not disclosed for reasons of
1180 privacy and data protection. Data from Envireau Water (2017a).

	UK Grid ref	Ground / wellhead elevation	Borehole depth	Open interval	Rest water level 20/4/16
		m asl	m bgl	m bgl	m asl
BHA	SE77153 79025	31.69 / 32.34	11.5	8.0 to 11.0 SUP/WKC	23.27
BHB	SE77099 78989	31.98 / 32.55	11.5	8.0 to 11.0 SUP/WKC	23.03
BHC	SE77162 78964	31.87 / 32.31	11.5	8.0 to 11.0 SUP/WKC	23.03
BHD	SE77132 78963	29.01 / 29.64	38.0	25.0 to 37.0 KC	22.38
BHE	SE 77110 78969	28.94 / 29.73	222.0	192.6 to 222 Corallian	26.72
G1		c. 22	c. 36	KC	
G2		c. 22	c. 24	SUP/WKC	
G3		c. 25	c. 50 ?	Most likely KC	
G4		c. 25	c. 50 ?	Most likely KC	
G5		c. 22	c. 5	SUP/WKC	
G6		c. 23	c. 21	SUP/WKC	

1181

Table 3a. Field determinations for surface waters. IQR = interquartile range; u/s = upstream, d/s = downstream; EC = electrical conductivity; ORP = oxidation-reduction potential; T = temperature. Eh is estimated from ORP on the basis of a Pt: Ag/AgCl electrode combination by adding 215 mV (Striggow 2013) and rounding to the nearest 10 mV. Data from S1 and S4 are skewed towards winter measurements as the watercourses were typically dry in summer.

		pH		EC (µS/cm)		T (°C)	
		Median	**IQR**	**Median**	**IQR**	**Median**	**IQR**
S1 Sugar Hill Drain d/s	27	8.09	7.68 to 8.19	745	668 to 833	8.5	6.3 to 10.6
S2 Costa Beck	18	7.65	7.37 to 7.89	552	519 to 572	10.2	7.3 to 14.3
S3 Ackland Beck	14	7.69	7.47 to 8.00	881	770 to 1018	10.6	7.0 to 13.4
S4 Sugar Hill Drain u/s	27	8.01	7.76 to 8.14	796	710 to 899	7.8	6.3 to 10.4
		ORP (mV		**Eh (mV)**			
		Median	**IQR**	**Median**	**IQR**		
S1 Sugar Hill Drain d/s	27	+97	+68 to +139	+310	+280 to +350		
S2 Costa Beck	18	+177	+128 to +216	+390	+340 to +430		
S3 Ackland Beck	14	+117	+41 to +172	+330	+260 to +390		
S4 Sugar Hill Drain u/s	27	+126	+71 to +143	+340	+290 to +360		

Table 3b. Laboratory determinations of selected parameters for surface waters. For each parameter, the upper row shows the median, the lower (feint script), the interquartile range. Amm-N = ammoniacal nitrogen (as N), nitrate cited as NO_3^-. N_1 = number of sample determinations. Data from S1 and S4 are skewed towards winter measurements as the watercourses were typically dry in summer.

Location		S1	S2	S3	S4
Solute hydrochemistry					
N		12	8	7	13
Ca	mg/L	121	86	116	124
		101-137	81-91	99-128	96-139
Mg	mg/L	7.0	7.1	10.1	7.3
		4.8-7.1	6.7-7.4	8.3-11.9	5.1-7.8
Na	mg/L	21	15	42	17
		16-24	15-16	34-61	13-20
K	mg/L	10.8	2.2	5.1	11.5
		8.3-13.0	2.1-2.3	4.3-5.8	8.1-14.1
Cl^-	mg/L	65	29	84	59
		57-75	28-30	71-101	46-71
SO_4^{2-}	mg/L	56	42	60	61
		45-61	38-44	37-60	44-72
Alkalinity	meq/L	5.1	3.9	5.6	5.0
		3.4-5.7	3.5-4.2	4.9-5.7	2.9-6.4
NO_3^-	mg/L as NO_3^-	19.1	25.6	7.0	22.1
		15.9-24.2	23.5-27.7	0.4-16.7	17.6-27.9
Amm-N	mg/L as N	0.05	0.09	0.06	0.05
		0.04-0.06	0.07-0.11	0.04-0.07	0.03-0.07
Fe	µg/L	84	88	33	93
		<20-163	53-106	<20-63	<20-309
Mn	µg/L	<2	12	19	2
		<2-3	6-13	4-42	<2-6
As	µg/L	<2.5	<2.5	<2.5	<2.5
		<2.5-<2.5	<2.5-<2.5	<2.5-<2.5	<2.5-<2.5
Ba	µg/L	111	68	80	113
		96-123	67-68	69-85	96-122
B	µg/L	38	17	34	37
		35-41	17-20	31-67	34-40
Sr	µg/L	237	143.5	254	267
		195-275	137-164	232-270	206-288
Dissolved gases					
N		11	8	7	13
CH_4	µg/L	<1	10.5	<1	11
		<1-<1	9.8-12	<1-8	<1-2
C_2H_6	µg/L	<1	<1	<1	<1
		All <1	All <1	All <1	All <1
CO_2	mg/L	38	27	40	32
		23-51	23-33	25-55	23-51

1216 **Table 4a. Field determinations for off-site groundwaters** (see legend to Table 3a). G1 consistently
1217 had an H_2S odour and exhibited effervescence. G2 had occasional H_2S odour. G2 and G5 also
1218 occasionally exhibited ferric oxyhydroxide 'flocs' in the water. Eh is estimated from ORP on the basis
1219 of a Pt: Ag/AgCl electrode combination by adding 215 mV (Striggow 2013) and rounding to the nearest
1220 10 mV.

1221
1222

	N	pH		EC (µS/cm)	
		Median	IQR	Median	IQR
G1 (Kimmeridge Clay)	30	7.60	7.47 to 7.69	2931	2881 to 2962
G2	30	7.54	7.46 to 7.64	890	880 to 906
G3	30	7.65	7.55 to 7.80	1535	1516 to 1559
G4	16	7.62	7.56 to 7.70	1068	1058 to 1087
G5	29	7.61	7.50 to 7.83	790	783 to 798
G6	16	8.08	7.93 to 8.25	939	786 to 1038
	N	ORP (mV)		Eh (mV)	
		Median	IQR	Median	IQR
G1 (Kimmeridge Clay)	30	-36	-82 to -18	+180	+130 to +200
G2	30	-28	-77 to +32	+190	+140 to +250
G3	30	+4	-23 to +64	+220	+190 to +280
G4	16	+87	-31 to +165	+300	+180 to +380
G5	29	+22	-16 to +73	+240	+200 to +290
G6	16	+155	+104 to +211	+370	+320 to +430

1223 **Table 4b. Laboratory determinations of selected parameters for off-site groundwaters.** For each
1224 parameter, the upper row shows the median, the lower (feint script), the interquartile range.

Location		G1	G2	G3	G4	G5	G6
Solute hydrochemistry							
N		8	8	9	9	8	8
Ca	mg/L	65	33	23	28	27	17
		61-71	32-34	22-24	28-28	27-28	16-19
Mg	mg/L	35	7.7	6.4	6.8	5.6	3.7
		31-36	7.4-7.7	6.2-6.6	6.6-6.9	5.5-5.7	3.3-5.5
Na	mg/L	642	163	362	244	149	178
		630-656	159-167	345-382	227-253	143-156	147-202
K	mg/L	6.1	3.0	3.7	2.9	2.7	2.6
		5.9-6.7	2.9-3.1	3.5-3.8	2.8-3.0	2.6-2.8	2.3-2.8
Cl^-	mg/L	100	29	49	25	22	20
		98-101	29-29	42-50	25-25	22-23	19-22
SO_4^{2-}	mg/L	820	29	157	84	19	46
		801-838	27-30	154-160	82-85	19-20	45-63
Alkalinity	meq/L	13.3	8.6	12.4	9.5	7.9	7.9
		12.7-13.8	8.5-8.8	12.0-12.6	9.3-9.6	7.9-8.0	6.4-8.8
NO_3^-	mg/L as NO_3^-	<0.2	<0.2	<0.2	0.8	<0.2	<0.2
		<0.2-<0.2	<0.2-<0.2	<0.2-1.6	0.4-1.0	<0.2-0.3	<0.2-<0.2
Amm-N	mg/L as N	2.34	0.73	1.20	0.64	0.68	0.06
		2.30-2.35	0.71-0.74	1.19-1.22	0.60-0.68	0.67-0.68	0.05-0.15
Fe	µg/L	410	1426	132	78	216	221
		347-551	1201-1700	128-143	30-88	157-280	79-1499
Mn	µg/L	5	330	38	221	282	25
		3-10	326-348	38-40	213-225	266-290	10-39
As	µg/L	<2.5	3.4	<2.5	2.4	<2.5	3.1
		<2.5-<2.5	2.6-4.7	<2.5-3.3	<2.5-4.9	<2.5-4.3	<2.5-3.9
Ba	µg/L	12	68	25	31	103	35
		11-14	67-70	24-25	31-32	100-106	22-59
B	µg/L	2334	472	1121	885	454	511
		2327-2369	466-487	1117-1129	880-903	444-456	454-765
Sr	µg/L	4019	509.5	742	426.5	399.5	181.5
		3901-4084	501-540	682-759	419-447	391-406	164-316
Dissolved gases							
N		8	8	8	8	8	8
CH_4	µg/L	620	19	3371	14	11	21
		572-706	18-23	2495-3527	13-15	9.8-12	10-50
C_2H_6	µg/L	<1	<1	19	<1	<1	<1
		All <1	All <1	<1-20	All <1	All <1	All <1
CO_2	mg/L	149	76	104	76	68	42
		139-158	70-81	91-107	73-79	62-75	34-55

1225

1226 **Table 5a. Field determinations for on-site groundwaters** (see legend to Table 3a). BHE typically
1227 exhibited effervescence on sampling, believed to be exsolution of methane. Eh is estimated from ORP
1228 on the basis of a Pt: Ag/AgCl electrode combination by adding 215 mV (Striggow 2013) and rounding
1229 to the nearest 10 mV.

1230

		pH		EC (µS/cm)		T (°C)	
		Median	**IQR**	**Median**	**IQR**	**Median**	**IQR**
BHA (Superficial)	42	6.74	6.56 to 6.87	1376	1174 to 1510	10.6	10.2 to 11.4
BHB (Superficial)	42	6.64	6.49 to 6.72	1610	1479 to 1708	10.9	10.1 to 12.4
BHC (Superficial)	41	6.68	6.53 to 6.73	1590	1476 to 1770	10.7	9.9 to 12.0
BHD (Kimmeridge Clay)	42	7.73	7.64 to 7.81	1738	1703 to 1796	11.2	10.5 to 12.3
BHE (Corallian)	42	9.78	9.68 to 9.87	3174	3126 to 3234	11.2	10.5 to 11.9
		ORP (mV		**Eh (mV)**			
		Median	**IQR**	**Median**	**IQR**		
BHA (Superficial)	42	-19	-41 to -4	+200	+170 to +210		
BHB (Superficial)	42	+24	+18 to +50	+240	+230 to +270		
BHC (Superficial)	41	+27	+19 to +48	+240	+230 to +260		
BHD (Kimmeridge Clay)	42	-148	-162 to -98	+70	+50 to +120		
BHE (Corallian)	42	-221	-258 to -101	-10	-40 to +110		

1231

1232 **Table 5b. Laboratory determinations of selected parameters for on-site groundwaters**. For each
1233 parameter, the upper row shows the median, the lower (feint script), the interquartile range.

Location		BHA	BHB	BHC	BHD	BHE
Solute hydrochemistry						
N		19	19	19	19	19
Ca	mg/L	302	354	380	42	0.8
		281-373	345-378	331-412	36-44	0.8-0.9
Mg	mg/L	18.2	7.4	12.7	6.3	0.9
		17.6-22.5	7.1-7.6	12.2-15.4	5.6-6.6	0.8-0.9
Na	mg/L	24	34	37	431	776
		24-26	33-34	33-38	402-459	712-786
K	mg/L	2.4	2.6	3.1	3.1	10.8
		2.3-2.5	2.5-2.7	3.0-3.3	3.0-3.2	10.5-11.1
Cl^-	mg/L	36	116	61	46	684
		34-36	112-124	59-61	44-46	666-694
SO_4^{2-}	mg/L	297	271	392	245	1.4
		256-478	267-284	362-537	241-250	0.8-2.3
Alkalinity	meq/L	8.8	8.5	9.1	12.9	10.9
		8.4-9.0	8.4-8.9	8.6-9.3	12.5-13.1	10.5-11.2
NO_3^-	mg/L as NO_3^-	<0.2	<0.2	<0.2	<0.2	<0.2
		<0.2-<0.2	<0.2-<0.2	<0.2-<0.2	<0.2-<0.2	<0.2-<0.2
Amm-N	mg/L as N	0.27	0.06	0.12	1.41	0.94
		0.26-0.29	0.05-0.08	0.12-0.13	1.37-1.42	0.92-0.99
Fe (diss)	µg/L	2696	659	1222	917	<20
		2348-2797	434-1321	932-1309	725-1116	<20-<20
Mn (diss)	µg/L	86	141	104	18	<2
		81-117	131-158	94-123	15-21	<2-<2
As	µg/L	<2.5	<2.5	<2.5	<2.5	<2.5
		<2.5-<2.5	<2.5-2.8	<2.5-<2.5	<2.5-2.6	<2.5-<2.5
Ba	µg/L	98	83	20	13	56
		77-115	80-85	19-22	12-13	52-58
B	µg/L	101	79	136	1583	250
		100-105	77-83	134-143	1561-1655	243-255
Sr	µg/L	534	499	567	765	131
		523-568	485-512	561-612	735-791	130-137
Dissolved gases						
N*		34	34	33	34	34
CH_4	µg/L	10	<1	2	68	50429
		9.0-11	<1-3	<1-5.8	58-80	41089-55815
C_2H_6	µg/L	<1	<1	<1	<1	8
		All <1	All <1	All <1	All <1	<1-9
CO_2	mg/L	296	341	350	102	7.4
		260-325	304-376	283-389	97-120	6.8-14

1252

Table 6. Statistical summary of $\delta^{13}C$ values for dissolved methane and carbon dioxide in sample sets from the Kirby Misperton area, with the laboratory's tap water and air as the laboratory's designated "controls". It is believed that the tap water methane isotopic ratio is likely to represent an equilibrated atmospheric content.

	N	$\delta^{13}C$ in dissolved methane (‰)			$\delta^{13}C$ in dissolved CO_2 (‰)		
		25%-ile	Median	75%-ile	25%-ile	Median	75%-ile
Laboratory tap water	12	-52.2	-49.5	-48.6	-13.0	-11.8	-10.8
Laboratory air sample	6	-50.1	-49.8	-49.4	-11.7	-11.2	-10.8
Samples with median dissolved methane < 10 µg/L							
S1	9	-49.8	-49.3	-47.4	-28.5	-26.7	-25.1
S3	7	-49.9	-49.0	-48.3	-26.6	-26.4	-26.1
S4	9	-50.4	-48.4	-47.5	-27.8	-27.0	-25.7
BHB	14	-54.7	-48.4	-46.4	-22.1	-21.8	-21.5
BHC	14	-53.2	-48.9	-47.5	-23.2	-22.9	-22.0
Samples with median dissolved methane > 10 µg/L							
S2	8	-56.3	-50.0	-49.1	-24.8	-24.3	-24.0
G2	8	-49.6	-49.1	-48.5	-27.0	-26.1	-25.3
G4	8	-49.4	-48.2	-46.7	-25.8	-25.7	-25.4
G5	8	-49.2	-48.0	-46.8	-26.3	-26.0	-25.8
G6	8	-49.5	-48.5	-45.9	-24.9	-24.1	-22.9
BHA	14	-55.4	-49.4	-47.8	-24.3	-23.9	-23.3
BHD	14	-52.2	-46.9	-46.1	-26.5	-26.0	-25.6
Samples with median dissolved methane > 100 µg/L							
G1	8	-65.5	-47.9	-43.8	-23.0	-22.6	-22.4
Samples with median dissolved methane > 1000 µg/L							
G3	8	-71.7	-59.0	-49.3	-25.4	-25.3	-25.0
BHE	14	-74.7	-71.9	-69.5	-13.2	-10.5	-8.2

FIGURE CAPTIONS

Figure 1. Simplified geological map of the Vale of Pickering, showing site location. (Based on information from British Geological Survey Geoindex viewer: contains public sector information licensed under the Open Government Licence v3.0).

Figure 2. (left) Map of Kirby Misperton area, showing study site and surface water sampling points S2 and S3; (right) diagram of KMA well site and groundwater / surface water monitoring points.

Figure 3. Construction of on-site monitoring boreholes BHA to BHE.

Figure 4. Scatter plots showing the correlation between primary and duplicate samples for dissolved methane, ethane and carbon dioxide. The dashed line shows a 1:1 correlation. Samples below detection limit are plotted at a value of half the detection limit.

Figure 5. Time series plot of dissolved methane concentrations in groundwater from selected locations during project lifetime (note logarithmic scale). Samples below detection limit are plotted at a value of half the detection limit.

Figure 6. Comparison of results of BGS method ("steel cylinder") and project methodology ("sealed glass vial") for dissolved methane sampling and analysis of groundwater from BHE.

Figure 7. Durov plot showing major ion composition of sampled waters. The meq proportions of major cations / anions are plotted on the triangular fields and then projected onto the central square field.

Figure 8. (top) Boxplots showing distributions of $\delta^{13}C$ in dissolved methane and dissolved carbon dioxide (numbers of samples in Table 6,) and (bottom) temporal variation is dissolved methane $\delta^{13}C$ in BHB, BHD and BHE. The isotopic composition of laboratory air is shown as a control.

Figure 9. A Bernard diagram showing fields typical of biogenic methanogenesis by CO_2reduction (red) and thermogenic (petrogenic) methanogenesis (blue), according to Baldassare (2010). Arrows show typical $\delta^{13}C$ ranges cited by Schloemer et al. (2016). Samples BHE and G3 are plotted, while the symbols for G1 represent the lowest possible molar $C_1/(C_2+C_3)$ ratio. The $C_1/(C_2+C_3)$ ratio is simplified to methane/ethane in this diagram, as no propane or higher alkanes were detected in the samples.

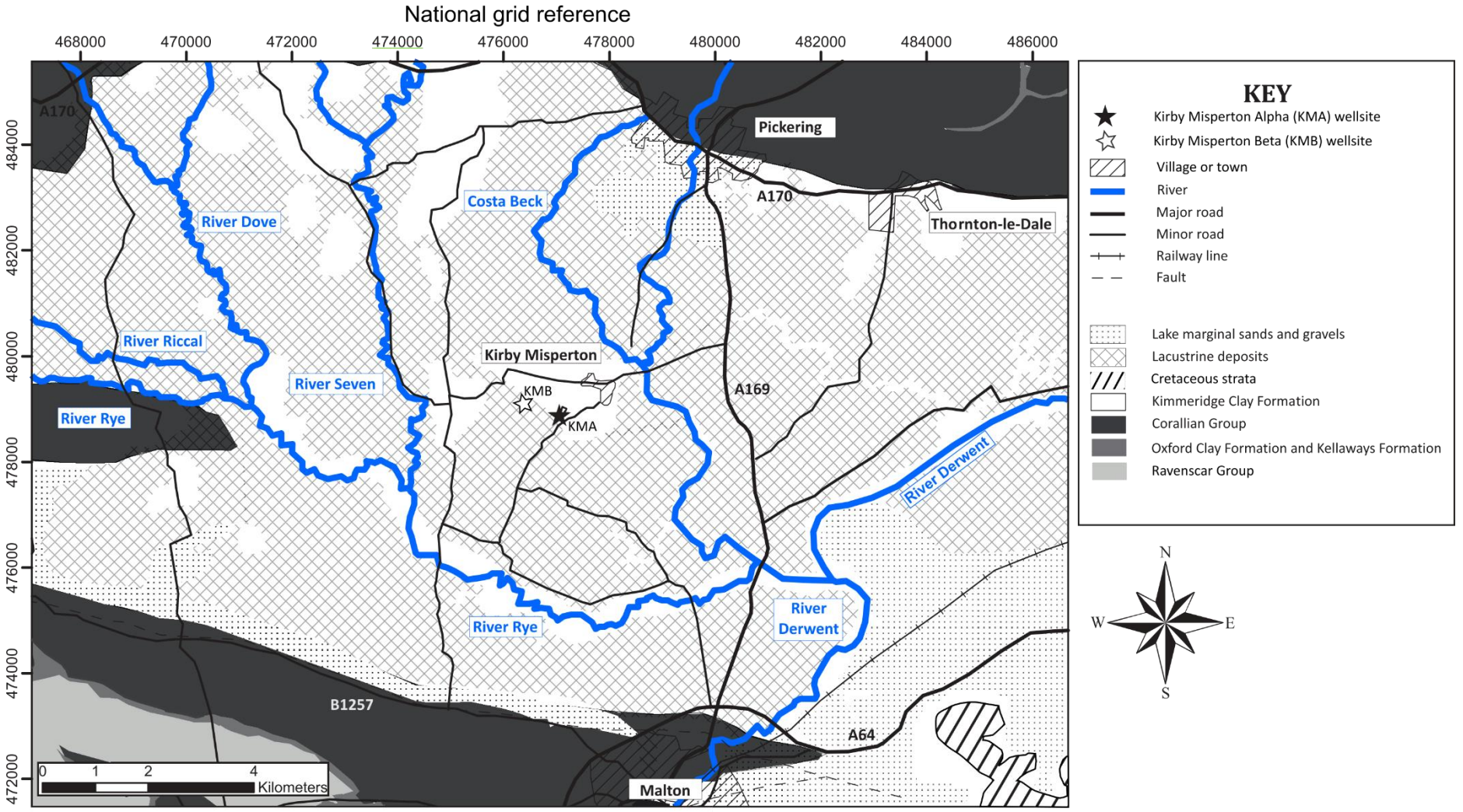

1285

1286 **Figure 1. Simplified geological map of the Vale of Pickering, showing site location.** (Based on information from British Geological Survey Geoindex viewer:
1287 contains public sector information licensed under the Open Government Licence v3.0).

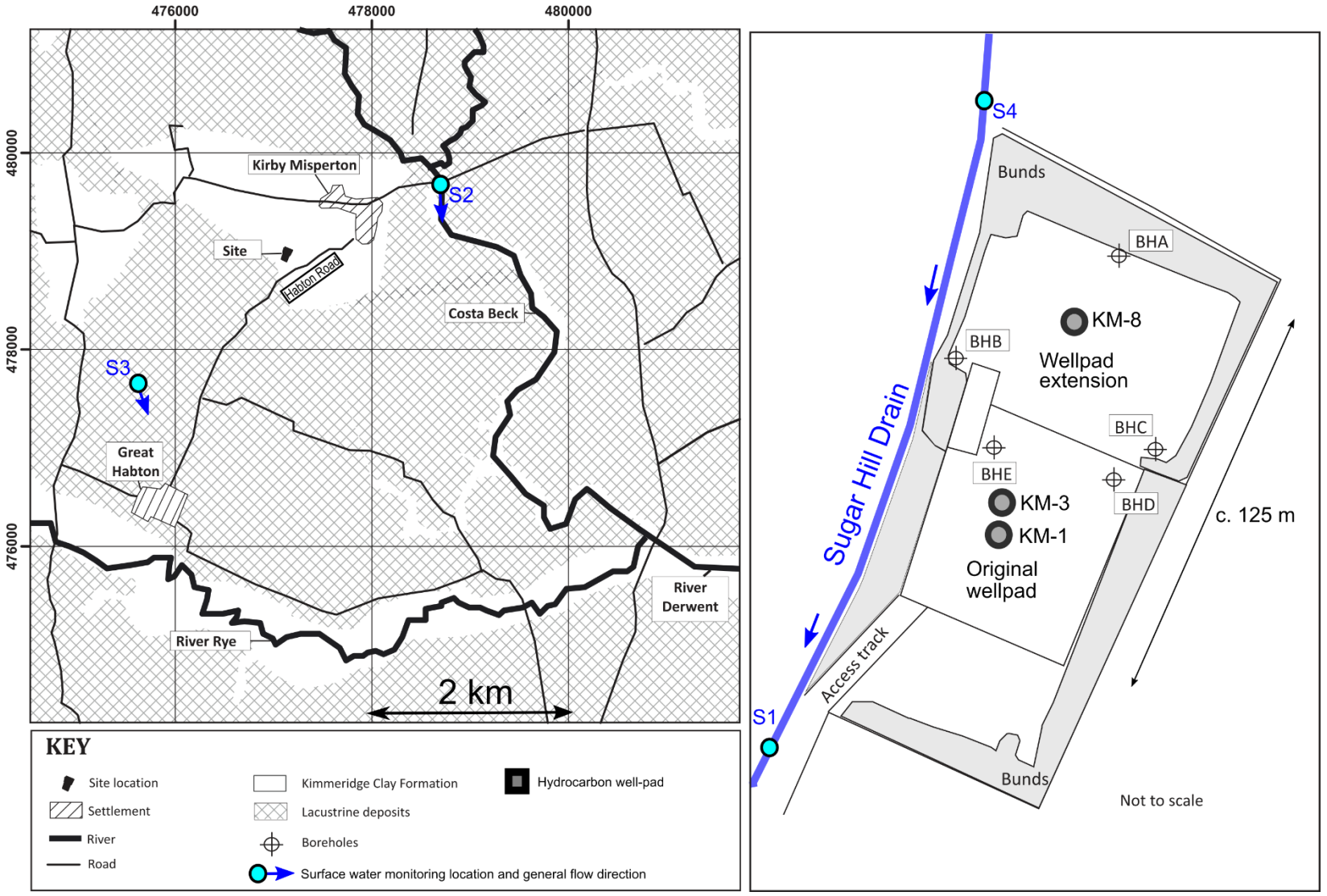

Figure 2. (left) Map of Kirby Misperton area, showing study site and surface water sampling points S2 and S3; (right) diagram of KMA well site and groundwater / surface water monitoring points.

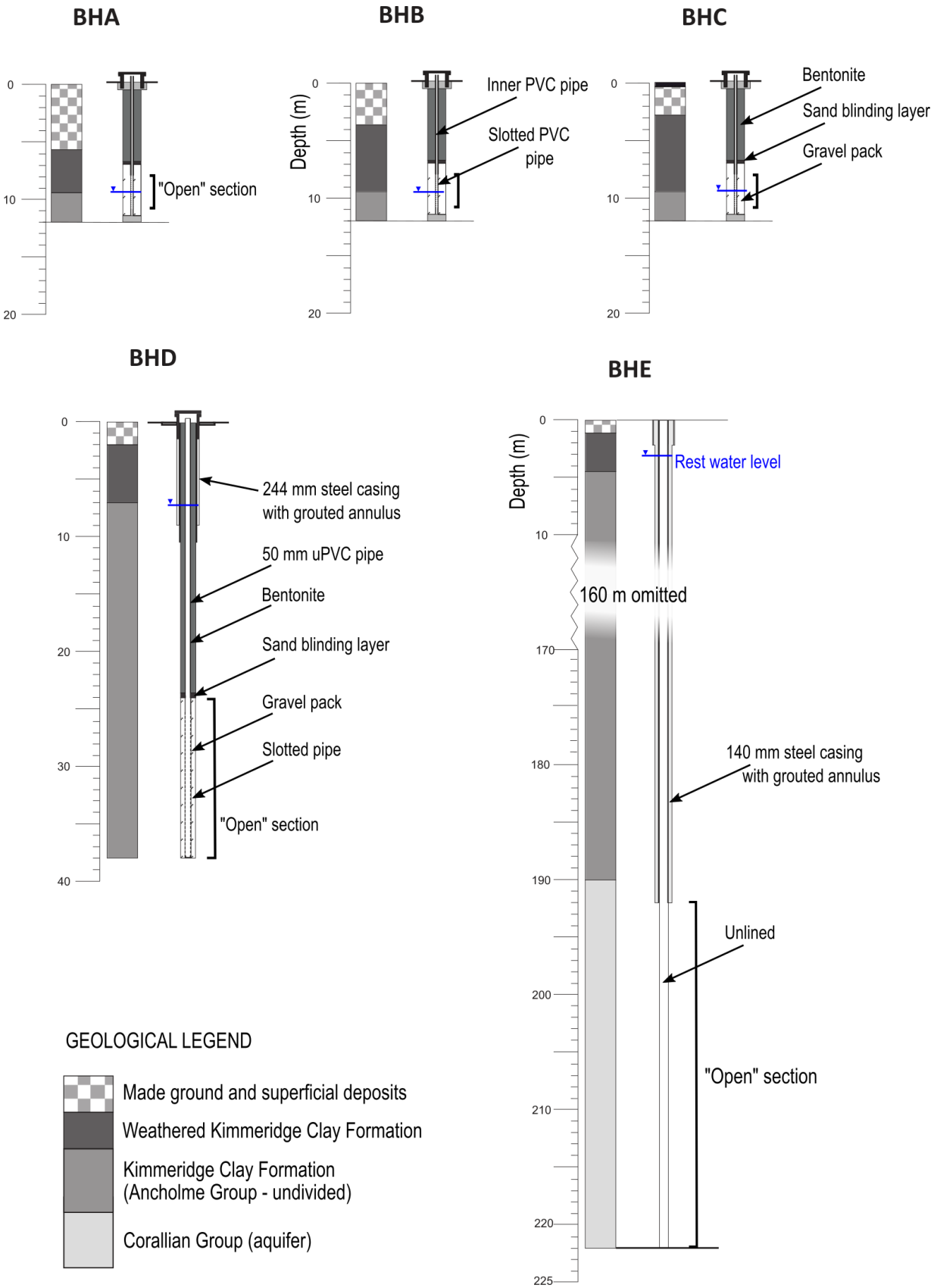

Figure 3. Construction of on-site monitoring boreholes BHA to BHE.

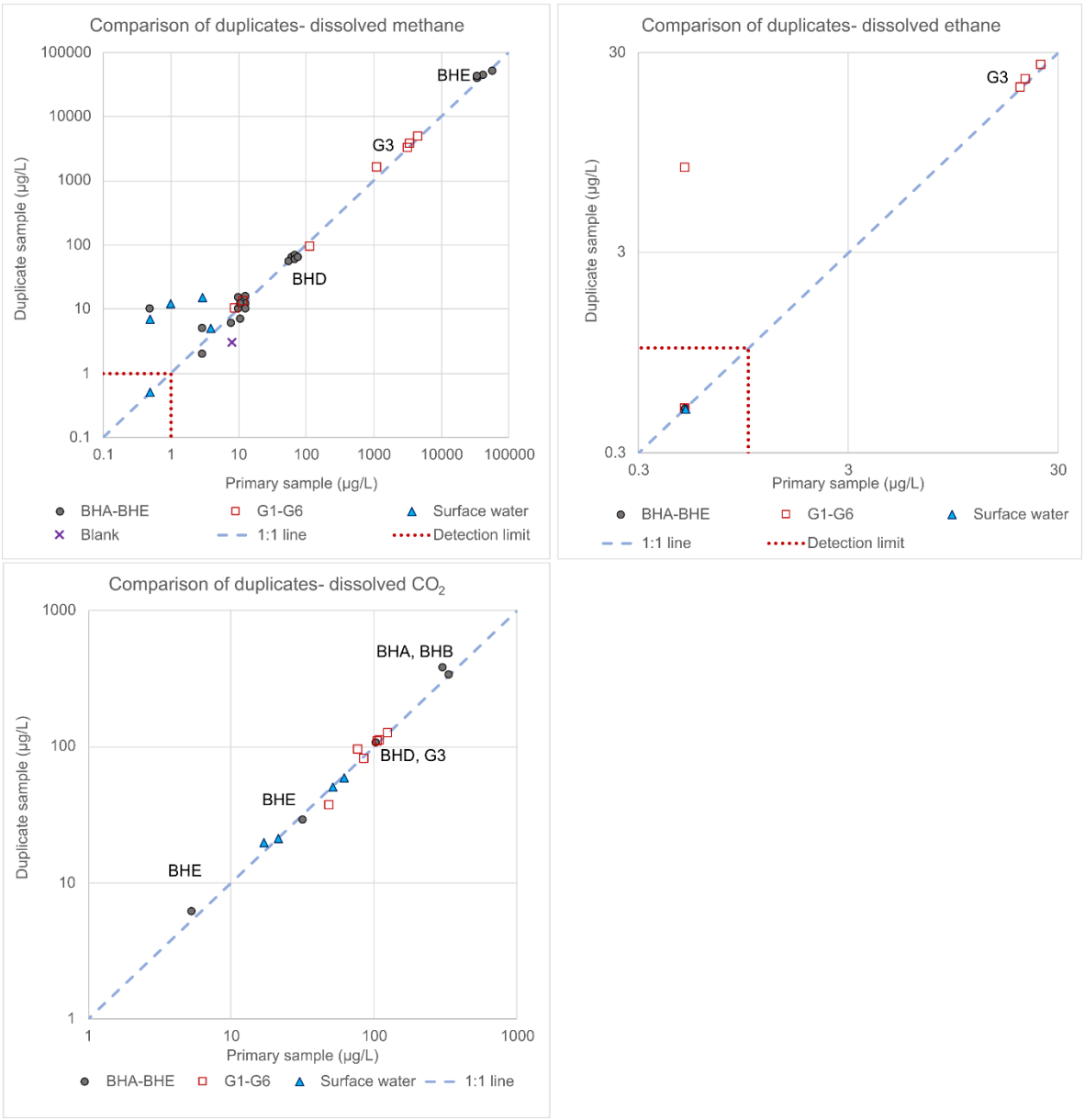

1294

1295 **Figure 4.** Scatter plots showing the correlation between primary and duplicate samples for dissolved
1296 methane, ethane and carbon dioxide. The dashed line shows a 1:1 correlation. Samples below
1297 detection limit are plotted at a value of half the detection limit.

1298

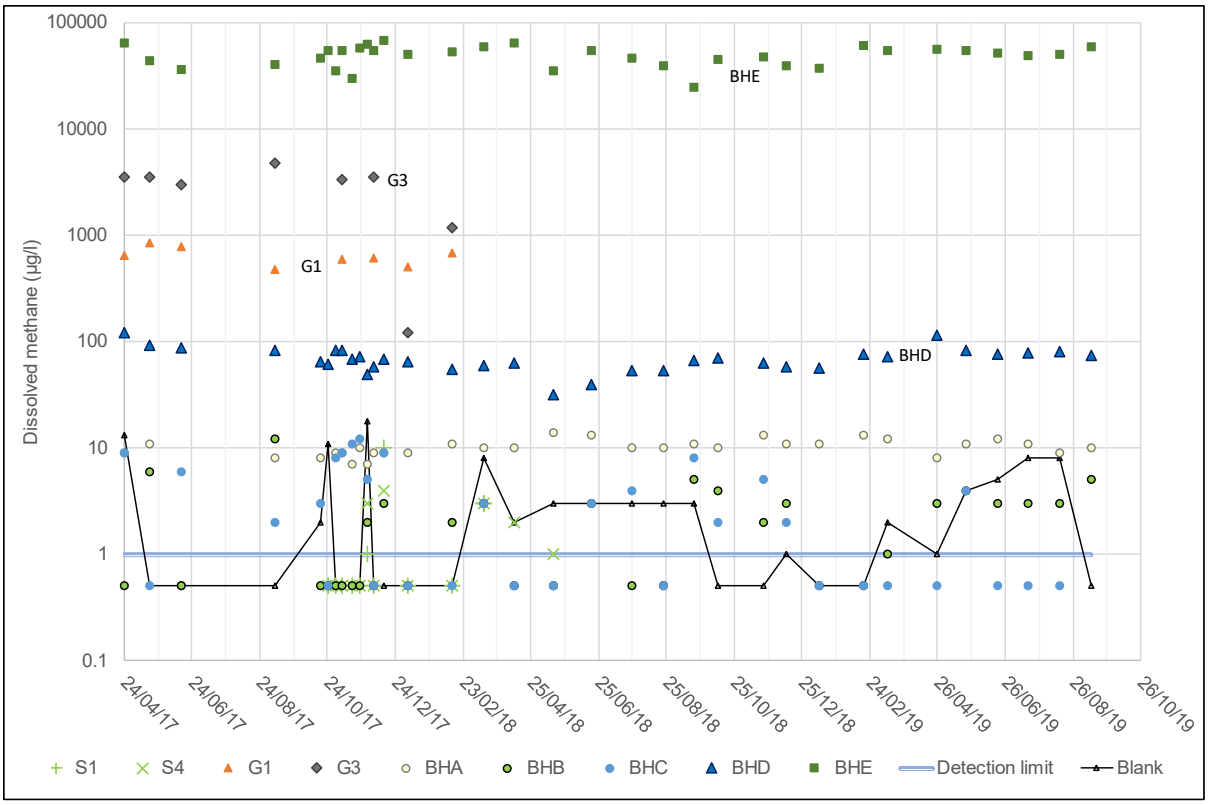

1299

1300 **Figure 5.** Time series plot of dissolved methane concentrations in groundwater from selected locations
1301 during project lifetime (note logarithmic scale). Samples below detection limit are plotted at a value
1302 of half the detection limit.

1303

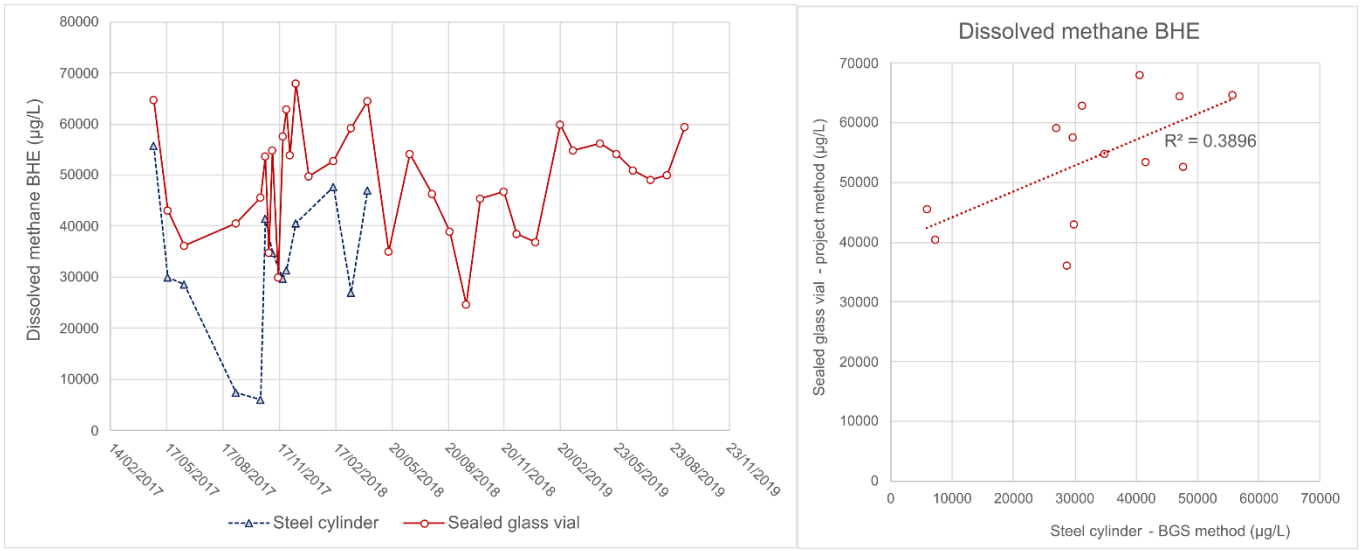

Figure 6. Comparison of results of BGS method ("steel cylinder") and project methodology ("sealed glass vial") for dissolved methane sampling and analysis of groundwater from BHE.

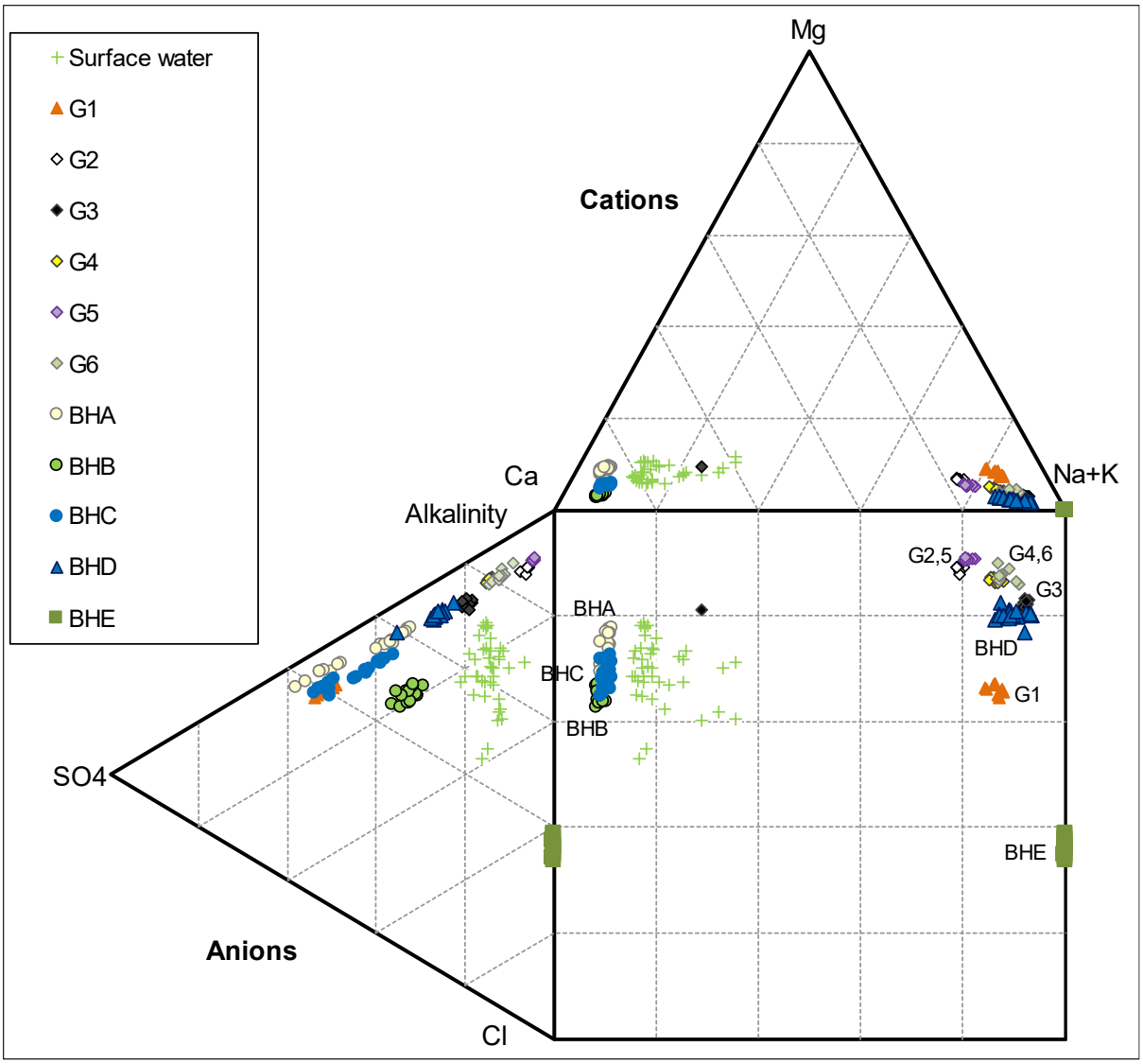

Figure 7. Durov plot showing major ion composition of sampled waters. The meq proportions of major cations / anions are plotted on the triangular fields and then projected onto the central square field.

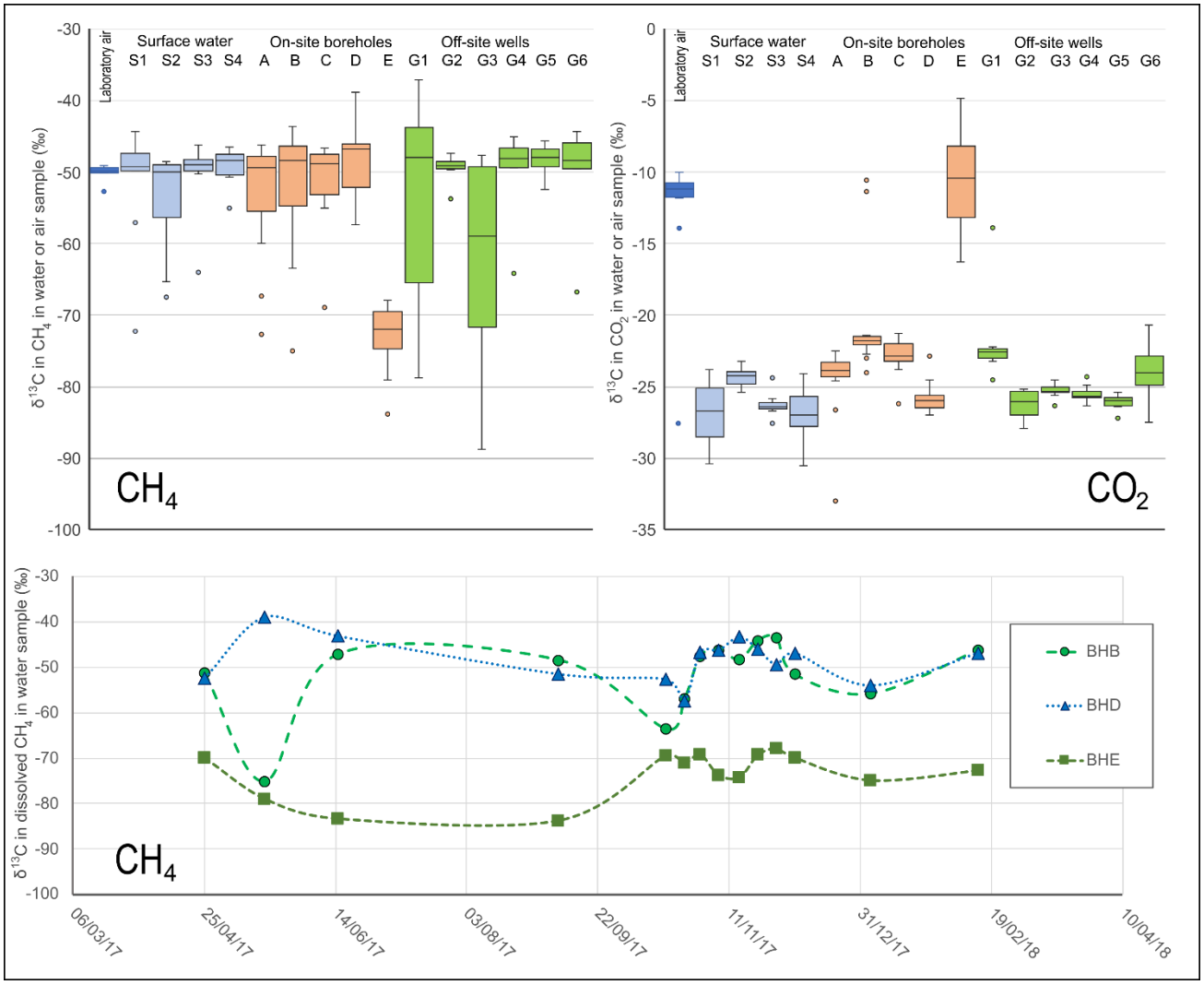

Figure 8. (top) Boxplots showing distributions of $\delta^{13}C$ in dissolved methane and dissolved carbon dioxide (numbers of samples in Table 6,) and (bottom) temporal variation is dissolved methane $\delta^{13}C$ in BHB, BHD and BHE. The isotopic composition of laboratory air is shown as a control.

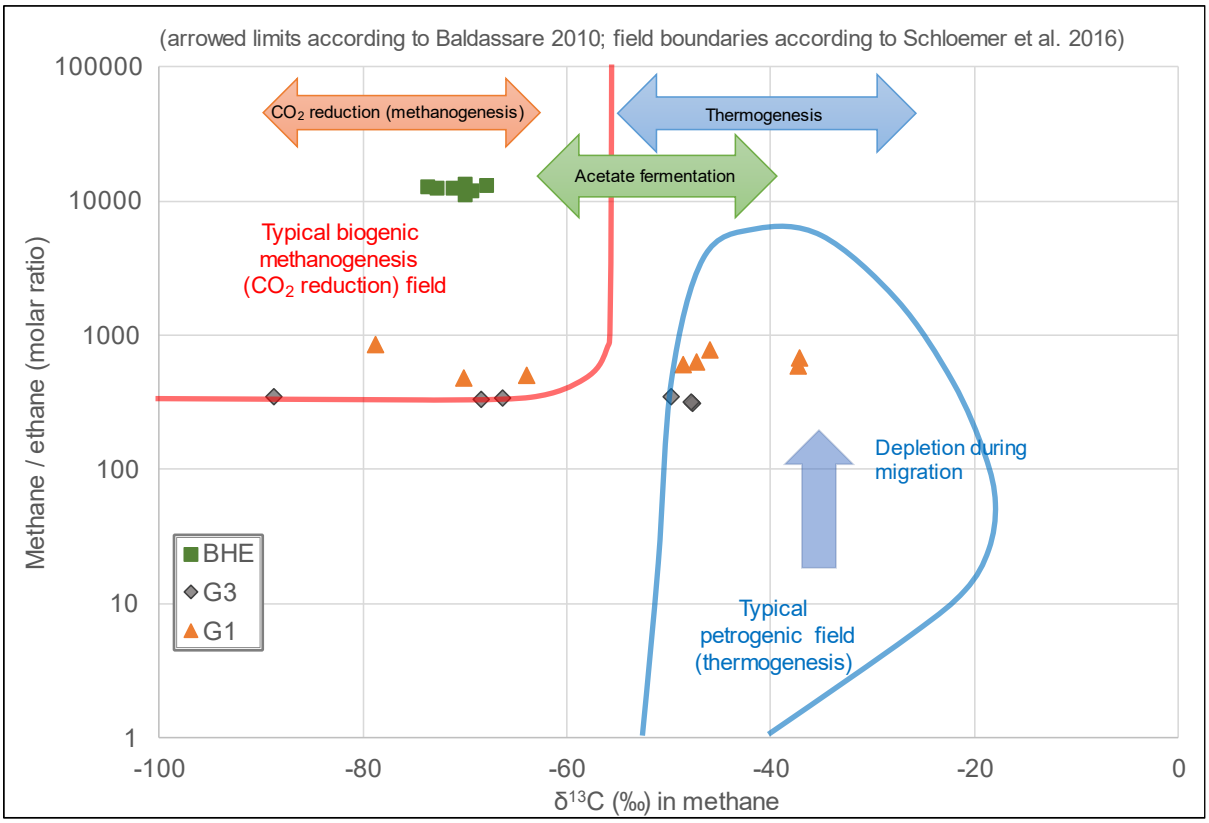

1317

1318 **Figure 9.** A Bernard diagram showing fields typical of biogenic methanogenesis by CO_2reduction (red) and
1319 thermogenic (petrogenic) methanogenesis (blue), according to Baldassare (2010). Arrows show typical $\delta^{13}C$
1320 ranges cited by Schloemer et al. (2016). Samples BHE and G3 are plotted, while the symbols for G1 represent
1321 the lowest possible molar $C_1/(C_2+C_3)$ ratio. The $C_1/(C_2+C_3)$ ratio is simplified to methane/ethane in this
1322 diagram, as no propane or higher alkanes were detected in the samples.

1323